12-2020

Synthesis, Characterization, and Application of Meso-Tetraphenyl Metalloporphyrin Photocatalysts under Visible Light

Alexis Echavarria
The University of Texas Rio Grande Valley

SYNTHESIS, CHARACTERIZATION, AND APPLICATION OF MESO-TETRAPHENYL METALLOPORPHYRIN PHOTOCATALYSTS UNDER VISIBLE LIGHT

A Thesis

by

ALEXIS ECHAVARRIA

Submitted to the Graduate College of
The University of Texas Rio Grande Valley
In partial fulfillment of the requirements for the degree of

MASTER OF SCIENCE

December 2020

Major Subject: Chemistry

SYNTHESIS, CHARACTERIZATION, AND APPLICATION OF MESO-TETRAPHENYL METALLOPORPHYRIN PHOTOCATALYSTS UNDER VISIBLE LIGHT

A Thesis
by
ALEXIS ECHAVARRIA

COMMITTEE MEMBERS

Dr. Jason G. Parsons
Chair of Committee

Dr. Erik Plata
Committee Member

Dr. Arnulfo Mar
Committee Member

Dr. Jose Gutierrez
Committee Member

December 2020

ABSTRACT

Echavarria, Alexis, Synthesis, Characterization, and Application of Meso-Tetraphenyl Metalloporphyrin Photocatalysts Under Visible Light. Master of Science (MS), December ,2020, 71 pgs, 48 figures, 9 tables, 66 references, 34 titles.

The photocatalytic activity of meso-Tetraphenyl Metalloporphyrins with different metal centers was investigated. The synthesized metalloporphyrin photocatalysts were performed and analyzed using FT-IR spectroscopy, UV-VIS spectroscopy, and powder X-Ray Diffraction analysis. The synthesized TPP crystals were determined to be tetragonal crystal structure and the structure was observed in all synthesized metalloporphyrin catalysts. The Soret (B) bands, Q bands, FT-IR functional groups were identified. Reaction progress was investigated by sampling at intervals of one hour and analysis of the samples was performed using Gas Chromatography-Mass Spectrometry. GC-MS analysis was used to identify the products of the photochemical catalytic redox reactions performed under purple light.

DEDICATION

The love and support of my family and my daughter have pushed me forward in every aspect of my life. I am very grateful for my amazing parents, my lovely seven-year-old daughter, and my once in a lifetime friends and mentors. The unconditional love I have for my daughter, Delilah Susana Echavarria, has made this milestone in my life possible and unique. Without you, my life would be different, this is for you to make you proud.

ACKNOWLEDGEMNETS

The respect and admiration I have for my mentors Jason Parsons and Helia Morales is immense. Thank you for your patience, support, encouragement, and knowledge you provided for me. Your mentorship made this milestone possible and my gratitude is the least I can give you.

To my friends and lab mates, thank you for all your support, your help, your friendship and all the great memories accumulated these past two years.

TABLE OF CONTENTS

LIST OF TABLES

Page

LIST OF FIGURES

Page

CHAPTER 1

BACKGROUND

History of Porphyrins

Porphyrins are heterocyclic tetrapyrrole aromatic organic molecules found in nature. Porphyrins and their derivative analogues such as metalloporphyrins and chlorines are highly colored compounds naturally present in living organisms including both plants and animals. The word porphyrin was derived from the Greek word porphyria, meaning deep purple or violet color. The intense color of the porphyrins is derived from the high amount of conjugation in the molecule, which allows the absorption of light in the visible region of the electromagnetic spectrum. The isolation of these compounds, especially the hematoporphyrin found in red blood cells responsible for oxygen transport in animals, and new synthetic routes have attracted tremendous attention to research on porphyrins, metalloporphyrins, and their analogues. Side groups of porphyrins are easily chemically modified due to their position on the porphyrin ring and electron density of the system. The chemical modifications and new synthetic schemes allowed for the development of fully synthetic tetrapyrrolic macrocycles such as phthalocyanines [1] and tetraphenyl porphyrin. Synthetic porphyrins and their derivatives are powerful tools for various applications, e.g., molecular electronics, artificial light harvesting, biomedicine, molecular recognition, also serving as building blocks for supramolecular assembly. [2] Porphyrin derivatives exhibit unique photophysical and electrochemical characteristics and allow for the creation of metalloporphyrins using various transition metals that bind to the porphyrin ligand through coordination of the transition metal and porphyrin ligand. The functionalization of the

metal center on to the porphyrin ligand enhances the properties of these compounds, enabling to acquire unique properties and perform vital roles in catalysis, molecular recognition, and sensing. These compounds, their analogues, and derivatives have major roles in biological reactions such as the transport of oxygen in mammals, photosynthesis in plants, protein synthesis, catalysis as cofactors and various proteins and many other vital processes required to maintain life. Tremendous research has been done regarding these compounds since the early 1940's covering their synthesis, chemical modifications, metal functionalization, as well as fully exploring the porphyrin compound's electrochemical and physiochemical properties. Over the years, researchers have successfully synthesized synthetic porphyrins such as metal phthalocyanines and synthetic metal meso-tetra tetraphenyl porphyrins that are a mimicking representation of nature's porphyrin. These synthetic derivatives carry the porphyrin core as their main structural framework and differing in the external substituents. These different substituents give rise to unique electrochemical properties associated with each porphyrin compound as well as the type of metal centers substituted into the porphyrin core, and the substituents surrounding the core. Therefore, the development of this new synthetic porphyrin compounds has propelled the research are of porphyrins to be fully explored in recent years, allowing the discovery and applications of many synthetic porphyrins that have the potential to mimic natural the natural occurring compounds.

Porphyrins in Nature

Porphyrin macrocycle are organic molecules very abundant in nature and these molecules are the catalytic basis of many biochemical reactions. The most common examples of natural porphyrins are hemes (found in hemoglobin, myoglobin, cytochromes, catalase, peroxidases), chlorophylls, and bacteriochlorophylls.[3,4] These molecules are responsible for biochemical oxidation and reduction reactions that make organisms function. Hemoglobin porphyrin found in red blood cells and myoglobin in the muscle tissues contain a heme group, which is constructed of porphyrin macrocycles as shown in Figure 1. The heme groups contain porphyrins that are substituted with various side groups. The most important role of heme porphyrins is to hold the metal center through coordination bonding through the nitrogen atoms in the ring to the iron (II) ion centers. For the proper function of hemoglobin iron coordination, which are key to the proper function of the porphyrins. The functionalization of metal centers in porphyrin such as iron found in the heme group allows the binding and distribution of oxygen in mammals.

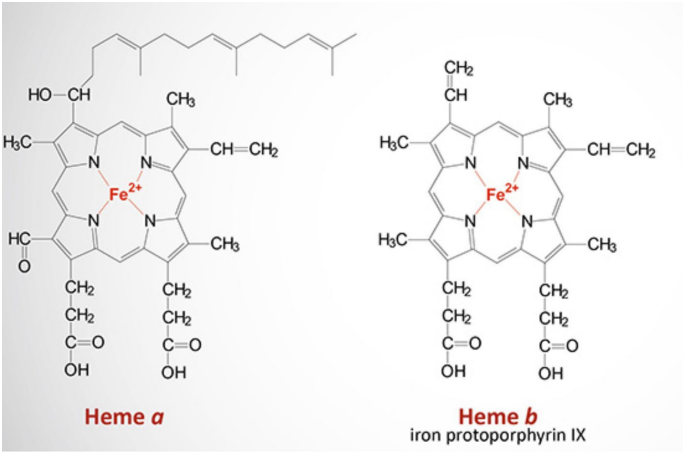

Figure 1: Porphyrin chemical structure of heme a and heme b. [62]

The chlorophyll photoreceptor contains a porphyrin system that holds a magnesium metal in the center. The magnesium center is responsible for its catalytic activity and performing photosynthesis. Similarly, to heme, the metal center is also held together in place through coordination through the nitrogen atoms in the porphyrin rings, forming coordinate bonds as well as electrostatic interactions between the metal centers and the available nitrogen atoms in the porphyrin ring system. There are four types of chlorophyll a, b, c, and d, but the main chlorophylls pigments are a and b. Chlorophyll a and b, differ only through having one methyl substituent in chlorophyll a, replaced by a formyl group in chlorophyll b[5] as shown in Figure 2.

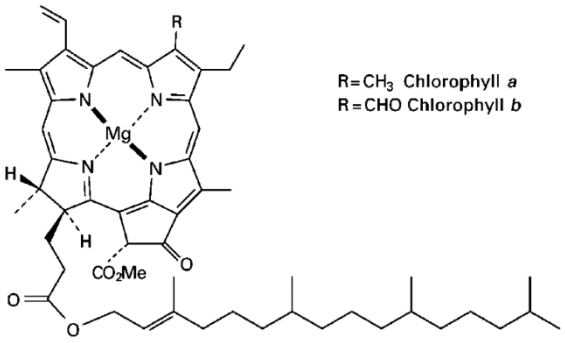

Figure 2: Chemical Structure of chlorophyll a and chlorophyll b[5]

Another metalloporphyrin is identified in cytochrome P-450 enzyme systems, which are in the liver of mammals and microbial organisms. These enzymes are responsible for the catalysis of a wide range of oxidation and reduction reactions responsible for detoxifying and eliminating harmful chemicals and their derivatives in biological systems. As well as these enzymes providing an indication of toxicity. Porphyrins can be considered biochemical indicators providing an indication of exposure to toxic chemicals or metals. Numerous studies during the past several decades have shown porphyrins and other constituents of the heme biosynthetic pathway may serve as sensitive and specific biomarkers of toxic metal exposures in human subjects. [6]

Furthermore, porphyrins are found in crude material such as petroleum as the result of the decomposition of the parent bio-material such as chlorophyll and micro-organisms.[7] Most crude oils contain traces of metal complexes of various forms including the porphyrins. The most abundant metal complexes present in organic portions of fossil fuel deposits are vanadium and nickel.[8] Vanadyl and nickel petroporphyrins were identified in fossil fuels as products derived from chlorophyll.[9,10] The most abundant types found in crude oil are etioporphyrins and deoxopylloerythroetioporphyrins.[11] Porphyrins provide markers for the origin and formation of petroleum. Over the years, petroporphyrin interest has increased to determine the role of these molecules in the formation of petroleum, their catalytic activities, as well a means to separate these type of metal complexes because they can reduce the activity of the catalyst in the hydrogenation process of petroleum.[12]

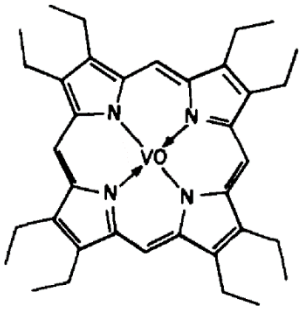

Figure 3: Chemical Structure of
Vanadyl Octaethylporphyrin[8]

The natural abundant presence of porphyrin macromolecules in nature gives researchers an indication of its roles. These porphyrin ligands and its metalloporphyrin derivatives have been shown to perform a variety of functions. The metalloporphyrin being the active center for nature's most vital functions such as the transport of oxygen in mammals, photosynthesis in plants, oxidation reduction reactions as a way of decreasing toxicity in biological systems, cofactors for essential vitamins such as B12, shown in Figure 4, and catalytic activities in the

formation of crude petroleum. These unique properties of porphyrins and their metalloporphyrin derivatives have promoted groundbreaking research in the past decades. Having explored the aspects and chemical properties of metalloporphyrins and their importance in nature, a new research area has been developed for the meso-tetraphenyl porphyrins with different metal centers, which have been synthesized, characterized, and used as potential photocatalysts for cross-coupling and oxidative reactions under irradiation using visible light.

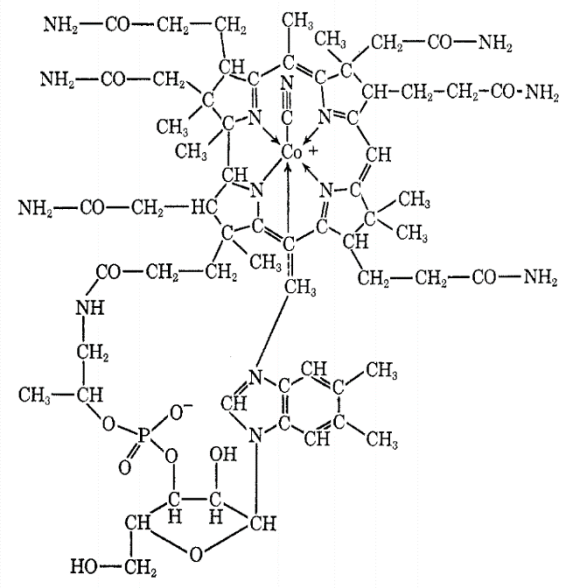

Figure 4: Chemical structure of Vitamin B12 [37]

CHAPTER II

INTRODUCTION

Metalloporphyrin Photocatalysts

As previously discussed, metalloporphyrin applications include sensitizers and catalysts such as their role in photosynthesis and respiration, and their unique photoelectronic properties makes them suitable as photocatalysts. Their strong absorption in the visible region makes them suited for catalysis of photo-driven redox reactions. Many of the roles of these photocatalyst include, but are not limited to: photo redox catalysis for hydrogen evolution from electron to proton sources combining hydrogen evolution, thermal redox catalysts for photocatalytic reduction of CO_2, oxygenation of substrates with H_2O and a redox catalyst for O_2 reduction, and photo redox catalysts for C-C bond formation reactions.[13] Visible light mediated photo redox catalysis is synthetic method which uses photo induced electron transfer (PET) to achieve chemical transformations. Photocatalysis offers advantageous protocols such as being environmentally friendly due to its mild reaction conditions.[14] Photocatalysis is based on the conversion of photo energy into chemical energy. The fundamental process of a metal-based photo redox catalyst is initiating a photon mediated excitation of the desired catalyst molecule transferring one electron from the t_{2g} to the π^* orbital of a highly conjugated ligand system to obtain the most stable-triplet-photo excited state. The excited state returns to the relaxed state by a single electron transfer process with the associated substrate molecule either through oxidation or reduction to promote the molecule for desirable organic transformation.[15,16]

Macrocyclic porphyrins which have a long conjugation network are suitable for

photocatalysts. Light induced photocatalysis needs to be accompanied with metal complexes with long-lived electronic excited state. The long-lived excited electronic state gives the catalyst different redox behaviors compared to their corresponding ground states. The metals commonly studied include the metals with a d^6 configuration, which include Ru (II), Re(I) Os (II), and Ir (II). The first row transition metals complexes have been shown to have short-lived excited states, which have been explored with metal complexes such as Cu (I), Cr (III), Fe (II) and Zn (II).[1718] One of the most utilized examples of a metal photocatalyst would be nickel based porphyrin catalysts which has been shown to have applications in cross-coupling reactions, photosensitizer properties, and its photo redox properties are still being explored.

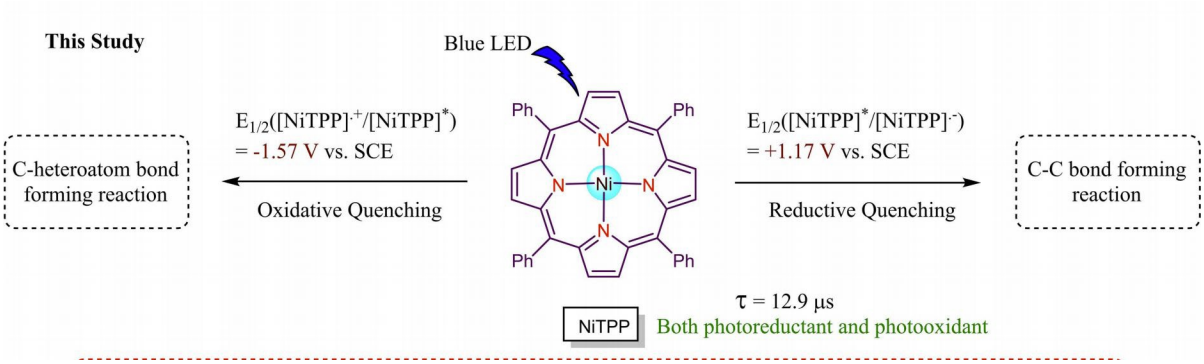

Figure 5: Nickle (II) Tetraphenyl porphyrin photocatalyst application as both photo oxidant and photo reductant [15]

A study performed by Mandal et al, exploring meso-tetraphenyl porphyrin ligand coordinated to Ni (II) show NiTPP as a photocatalyst having dual excited state redox properties: Oxidative Quenching and Reductive Quenching. NiTPP exhibits the dual activity of both excited state photo-oxidant and photo-reductant.

Reductive quenching, in simple terms, is the process by which the photocatalyst ,NiTPP, absorbs the irradiated light. There is an excitation of the photocatalyst from the ground state to the excited state, enabling the photocatalyst to interact with the substrate molecules through

adsorption if the substrate. This interactions sparks a single electron transfer, that occurs between the photocatalyst and the substrate. In reductive quenching, the single electron transfer occurs from the electron rich substrate molecule to the excited photocatalyst, setting off a series of steps that allow chemical transformation of the substrates involved in the chemical reaction. Eventually, the photocatalyst transfers the electron back to the available present molecules in its chemical environment, in most cases oxygen, creating a superoxide molecule as seen in Figure 6.

On the other hand, oxidative quenching starts by the excitation of the photocatalyst through light irradiation, exciting the photocatalyst from the ground state to the excited state. The photocatalyst interacts with the substrate molecule, making the single electron transfer possible. In this case, the single electron transfer happens from the electron rich photocatalyst to the substrate molecule, setting off a series of steps responsible for the desired chemical transformations. The electron deficient photocatalyst will eventually recover the electron back through another single electron transfer by interacting with the intermediates or molecules in the chemical reaction, starting the cycle all over as seen in Figure 7.

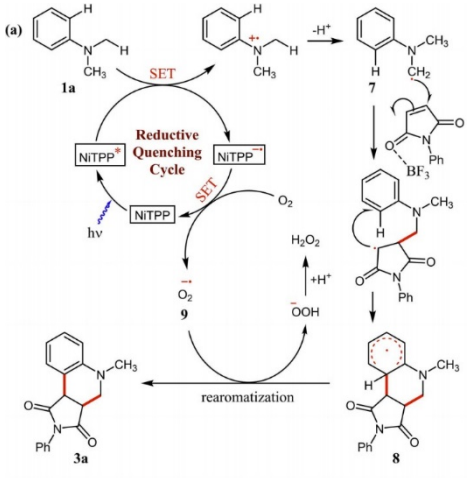

Figure 6: Proposed Mechanism and Control Experiment for NiTPP photocatalyst for Reductive Quenching Pathway[15]

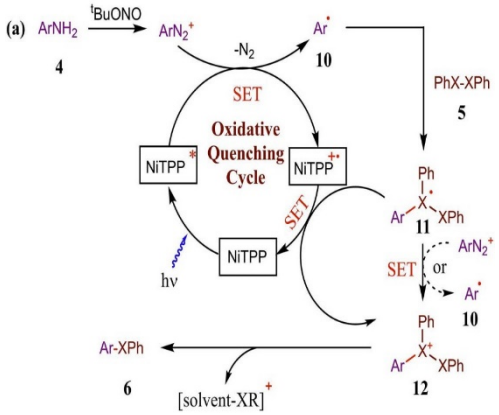

Figure 7: Proposed Mechanism and Control Experiment for NiTPP photocatalyst for Oxidative Quenching Pathway[15]

Structure

Porphyrins are derivative from the parent macrocycle porphine. The porphyrin skeleton is a tetrapyrrole macrocycle composed of four pyrrole subunits, which is the free base parent compound. Porphine is bond together through methine bridges at their α carbon positions, joining the four pyrrole rings together, resulting in two pyrrole (-NH) units, two pyrrolenine (=N) units, as well as 11 double bonds. All porphyrins have the same structural framework; however, they can be modified and contain various substituents on the meso carbon positions and beta carbon positions.[19,20]

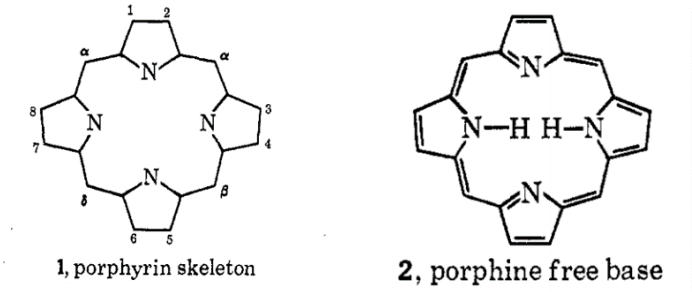

Figure 8: 1. Porphyrin skeleton structure
2. Free Base Porphyrin structure

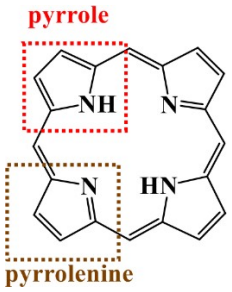

Figure 9: Pyrrole and Pyrrolenine location in the porphyrin structure

Porphyrins and their derivatives in the tetrapyrrolic macrocycle family are the most studied. The derivatives such as chlorins, bacteriochlorins, and isobacteriochlorins are shown below as well as the number of electrons associated with the macrocycle's aromaticity.[21]

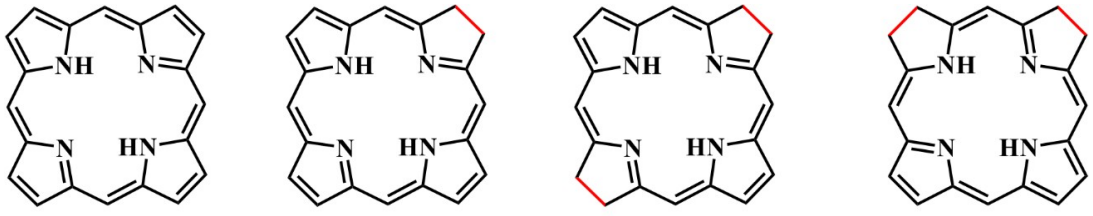

Figure 10: From left to right: Porphyrin, chlorine, bacteriochlorin, and isobacteriochlorine.

Porphyrin modification with different substituents can be achieved at the beta carbons (positions 2,3,7,8,12,13,17,18) or on the meso carbons (positions 5,10,15,20) as shown in Figure 11.

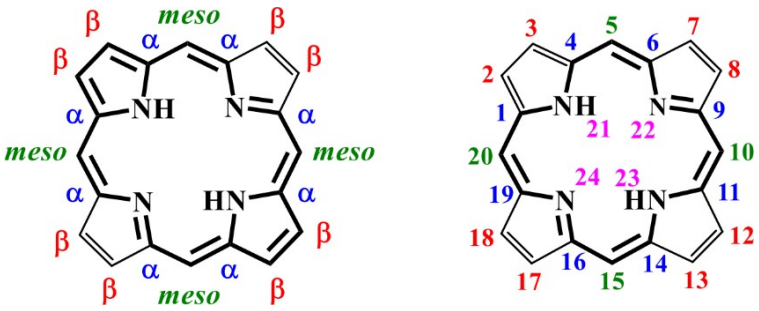

Figure 11: IUPAC numbering and naming of porphyrin positions

The unique structure of the porphine macrocycle ring system offers unique properties for the macrocycles like being able to accept protons to form a di-cation due to the two nitrogen atoms in the center of the ring, which have a lone pair electrons available to accept protons. [22] On the other hand, the porphine ring system is also able to form a di-anion due to the two NH groups losing a proton. The formation of this di-anion allows for porphyrin metalation and functionalization of many transition metals. The complex obtained by this process are referred as a metalloporphyrin and can take a different geometry corresponding to the nature of the metallic ion that is functionalized in the porphyrin system.[23,24]

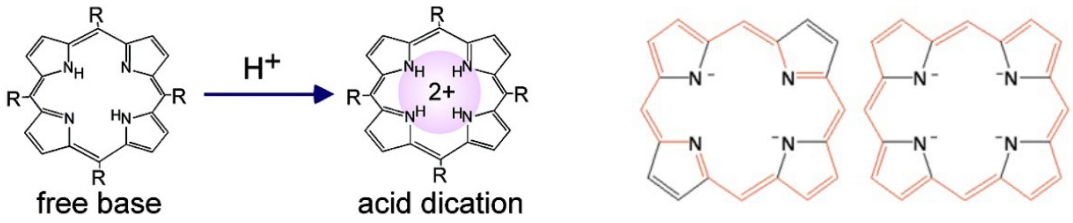

Figure 12: Formation of porphyrin acid di-cation (left) and di-anion (right)[22,23]

Porphyrin Derivatives, Porphyrinoids, and Phthalocyanines

Further chemical modifications to the porphyrin ring on the meso and beta positions creates new complexes that exhibit unique characteristics making porphyrin derivatives widely accessible to different areas of interest. These new characteristics can be used in applications such as optoelectronics, photosynthesis mimicking, medical applications, photosensitizers, catalysis, and many more. [25-28] These new derivatives are classified as porphyrinoids as shown in Figure 13. Examples of porphyrinoids include calixpyrroles[29], contracted and expanded, heteroatom-exchanged, and inverted porphyrinoids.

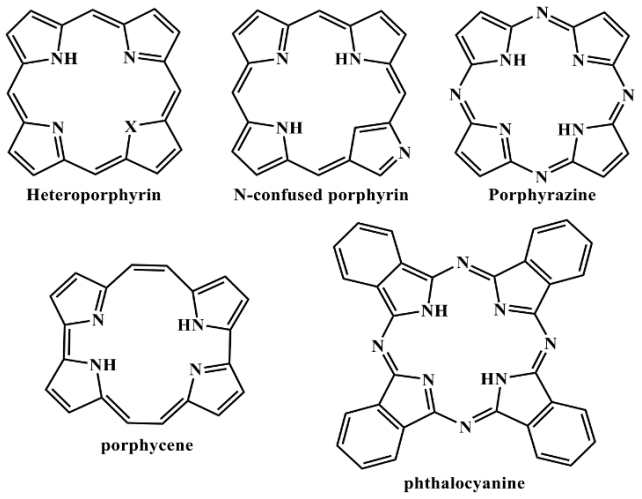

Figure 13: Synthetic porphyrinoids and porphyrin derivatives chemical structures

Core modifications have also been explored and implemented by either replacing individual pyrrole units or by elongation of the π-conjugation system of the porphyrin core.[30,31] Elongation is achieved by fusing polycyclic aromatic ring at the edge of the macrocyclic core which has resulted in a new class of porphyrinoid called phthalocyanines.[32] Phthalocyanines,

since their discovery in 1907 as a minor byproduct of the synthesis of *o*-cynobenzamide, have been extensively studied due to high physical and chemical stability. Furthermore, its metal complex, copper phthalocyanine, was first synthesized in 1927; while iron phthalocyanine was accidentally discovered the following year. [33] Another synthetic compound derived from porphyrin is tetraphenyl porphyrin (TPP). TPP is a thermally stable ligand, which is easily synthesized through a couple of well-established synthetic methods.[34] TPP and its metal complexes have been greatly researched due to its stability and versatility in its applications. TPP is related to naturally occurring porphyrins by having the same macrocyclic skeletal structure, consisting of four pyrrole groups alternately linked through methane bridges.

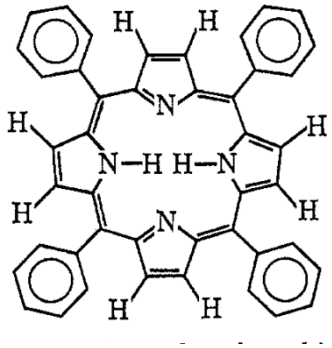

Figure 14: Tetraphenyl Porphyrin (TPP) free base ligand chemical structure

Porphyrin and its derivatives have unique properties that allows them to accept and bind a transition metal in the center of the porphyrin ligand, creating new complexes called metalloporphyrin. Porphyrins and their metal complexes have been extensively researched through their versatility induced by their coordination chemistry, since they can act as a ligand for cations as free base, or ion carriers for anion binding. The four nitrogen atoms present in the porphyrin ligand have the most versatility as chelating systems, since a majority of transition metals have been coordinated to the porphyrin system.[35] The chemical ability of the porphyrin

system to form a di-anion, which allows for metal functionalization and coordination into the porphyrin core, thus taking on different geometries depending on the nature of the metal center ion. These porphyrins are the active component in its biological system or in some way they ultimately connect to the activity of the system. Many of these systems ultimately differ in their behavior and this is the result of:

(a) the effects of a central metal ion on the π-bonding system of the porphyrin ring,

(b) the ease in which the porphyrin ring can assume various planar conformations,

(c) the chemistry and stereochemistry of side chains of the porphyrin ring, and

(d) the general molecular environment of the porphyrin in a certain biological system.[36]

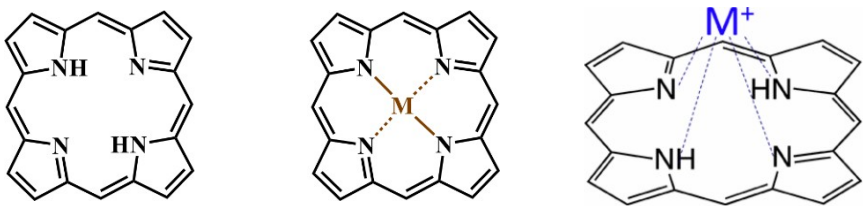

Figure 15: From left to right: General structure for free base porphyrin, metalloporphyrin, and porphyrin binding mechanism of cation.

Further exploring the advanced structural nature of the porphyrin ring system lets scientist understand the photophysical properties, such as visible absorption spectra, solubility, and magnetic properties, as well as clarifying its unique chemical properties the porphyrin compounds. Knowledge of the porphyrin structure clarifies its chemical features such as the rates

and mechanisms of metalloporphyrin formation and decomposition, ligand reaction at the metal center of the metalloporphyrin, substitution reactions on the ring system, and oxidation-reduction reactions of the porphyrin and metalloporphyrin system.[37] X-ray crystallography data has been a breakthrough in being able to determine the crystal structure of the porphyrin ring and porphyrin like compounds. One problem that arose in the porphyrin structure was determining the position of the hydrogens that saturate two of the four nitrogen present in the porphyrin core. It has been established that the inner pyrrole hydrogens are opposite of each other, not adjacent to each other and are not shared equally among the four nitrogen atoms such as illustrated in Figure 16:

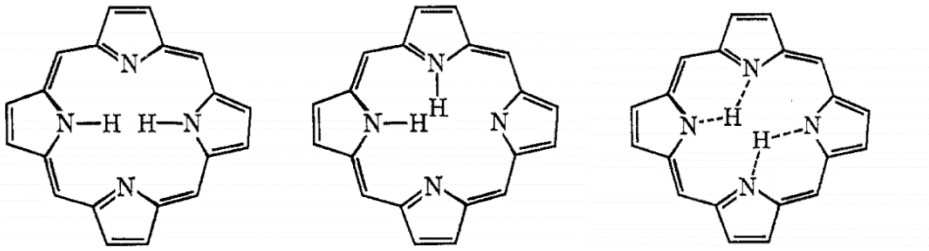

Figure 16: Hydrogen location in the porphyrin core. From left to right: correct positioning of the pyrrolic hydrogens, adjacent hydrogens, and shared hydrogens in porphyrin core.

Further examining the chemical structure of the porphyrin ring, researchers have been able to discover that the bond distances of the porphyrin ring are quiet constant and small changes in the distances and bond angles are attributed to the effects of different substituents to attached to the porphyrin skeleton. However, these differences are usually smaller than the estimated errors of the best bond parameters of the determined structure, not allowing any variations in these parameters as illustrated in Figure 17.

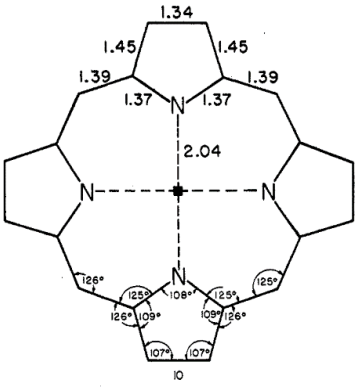

Figure 17: General porphyrin bond lengths and angles

The fixed distance from the pyrrole nitrogen to the centers of the ring is approximately 2.04 angstroms. However, this distance can vary in the metalloporphyrin's depending on the metal center. For example, in the ferric porphyrins the distance from the pyrrole ring to the metal center is found to be approximately 2.10 angstroms, whereas the distance in nickel porphyrin are approximately 1.95 Å. Researcher observed the variations of the metal to pyrrole-nitrogen distance, or M-N distance. The M-N distance depends on the macrocyclic nature of the porphyrin ligand and the atomic radii of the metal center. The M- N distance in the phthalocyanine compounds is about 0.05 angstroms smaller than in the metalloporphirins.[38] The change in M-N distances is exemplified by the M-N in copper (II) phthalocyanine is 1.93 Å compared to the distance of copper tetraphenyl porphyrin which is 1.98 Å. The macrocyclic nature of the porphyrin ligand can explain some of the M-N distances assuming the nitrogen to center of the ring distance is a fixed distance and the macrocycle cannot easily contract or expand to be able to functionalize the different metal atoms, instead the ligand accommodates by

projecting the metal center above the plane and the M-N distances become closer. The observed small increase in the M-N bond distances from 1.96 Å of nickel (II) porphyrin to 2.00 Å in palladium (II) porphyrins even though their atomic radii are 0.72 and 0.82 Å, respectively exemplifies the structure. Phthalocyanines also follow this pattern, M-N distance in copper (II) phthalocyanine is 1.94 Å while the platinum (II) phthalocyanine has a M-N distance of 1.98 Å, while their atomic radii of these two atoms are 0.73 and 0.82 Å, respectively.

Porphyrin synthesis and modifications are what determines the properties of each compound. As discussed, porphyrins and their derivatives have promising applications in photocatalysis. The effectiveness of the porphyrin photocatalysis is determine by electron density of the porphyrin system, the substituents chemically bonded to the porphyrin core, as well as the type of metal that is substituted into the porphyrin core. The substitution of the metal into the system forms the metal substituted complexes that are essential for photocatalysis. The nature of the metal bonded through coordination of the core and metal gives rise to other unique properties of these compounds. This also changes physiochemical and electrochemical properties of the porphyrin compounds. Many of the natural occurring porphyrins found in nature have a coordinated metal center in the porphyrin core which is a clear indication of the vital role that it plays in the effectiveness of the porphyrin compound. Metalloporphyrin complex formation and the geometries of the complexes will be further explored.

Metalloporphyrin Coordination and Geometry

Metalloporphyrin metal coordination and geometry differ depending on the nature of the metal center and the type of porphyrin compound. The porphyrin ligand forms a di-anion by losing two pyrrole protons through complexation of metal ions and acts as a tetradentate ligand in most cases. Thus, the usual minimum coordination number for the porphyrin ligand is four, however; it can adopt several coordination structures above four. Metalloporphyrins form compounds in which the metal may be four-coordinated, five-coordinated, six-coordinated, or eight-coordinated. Four-coordinated compounds have a square-planar geometry which is the case for most of metalloporphyrins and metal substituted phthalocyanines. These compounds have a square-planar coordination with the metal ion in the plane of the four-pyrrole nitrogen and contain no axial ligands. The four-coordinate system is considered the simplest derivative observed for most metals, the first transition series and divalent metals have been synthesized and characterized.[39]

Coordination numbers greater than four is the result of additions of additional ligands, whether they are neutral or anionic in nature. There are several five-coordinated metalloporphyrins with a tetragonal pyramid geometry as well as square-pyramidal geometry, such as the high-spin and low spin ferric porphyrins as discussed by Hoard et al,[38] as well as the vanadyl-substituted etioporphyrin,[40] and this coordination is also present in similar compounds such as magnesium phthalocyanine hydrate.[41] The five coordinate complexes have a square-pyramidal geometry with a single axial ligand occupying the apex of the square pyramid as illustrated below as well as having the metal center projected out of the porphyrin plane with variations in length (a). One of the most important characteristics of this structure is the displacement of the metal atom out of the

porphyrin plane which allows relatively large M-N bond distances without requiring large, energetically radial expansion of the porphyrin core.

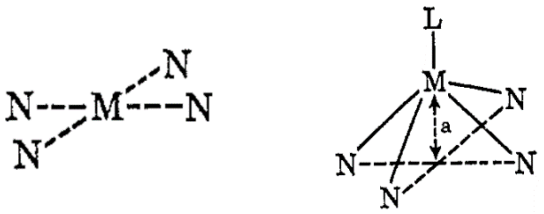

Figure 18: General Four-Coordinated square-planar metalloporphyrin structure (left) and Five-Coordinated tetragonal pyramid metalloporphyrin coordination (right)

In addition, there are possible macrocyclic metalloporphyrin and metal substituted phthalocyanines that have adopted a six-coordinate complex such as rhodium carbonyl tetraphenyl porphyrin chloride[42] which has the coordination structure of a distorted octahedral geometry shown in Figure 19. The two axial ligands of the six-coordinate metalloporphyrin are found on opposite sides of the porphyrin plane, resulting in tetragonal geometries. The two ligand donors could be allocated on the same side of the plane, however; no complex has been characterized with this structure. The majority of six-coordinated metalloporphyrin are first-row transition metals derivatives. These coordinated porphyrins contain equivalent axial ligands. The coordination can be considered as a prototype for the coordination that the majority of the porphyrin found in nature adopt, such as the cytochrome systems and hemoproteins found in biological systems. When the metal is out of the porphyrin plane, metalloporphyrins adopt a possible seven-coordinate system. Another possible, yet rare coordination complex would be an eight- coordinated complex, which forms a “sandwich complex” with a square-antiprismatic geometry. This eight-coordinated complex is formed between two phthalocyanine rings and a stannic ion.[43]

The seven coordinated complex has three axial ligands and the general structure contains two ligands in the same side as well as an opposing ligand on the other side of the porphyrin plane. The eight- coordinate porphyrin complex is usually formed when the metal center is located between two porphyrin or phthalocyanine monomers forming a sandwich or bridge dimer and creating a square-antiprismatic geometry such as the stannic complex illustrated Figure 19. The different coordination of these complexes depends on the electronic configurations of the metal ions. The different nature of the metal centers creates variety in lengths of the M-N distances, dihedral angles, and coordination of the complex. The macrocyclic constraints of the porphyrin core also play a role in the formation of the complex and length of the M-N bond distance by subrationally stretching it. The disruption of the pi delocalization within the porphyrin macrocycle would lead to greater flexibility of the M-N bonds and distances.

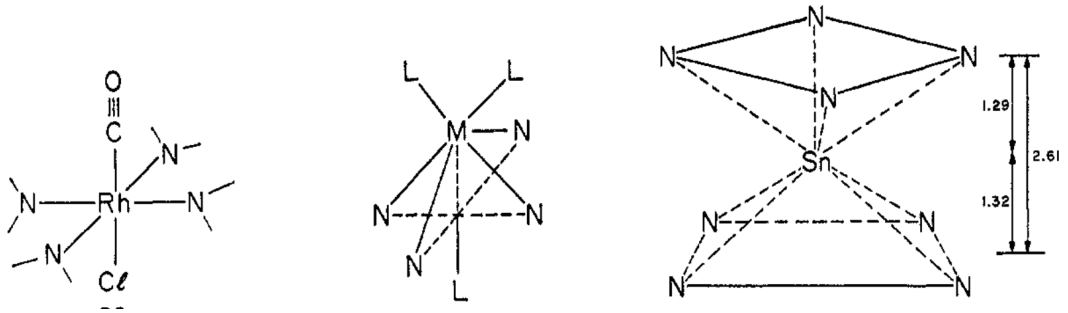

Figure 19: Six-coordinate metalloporphyrin (left),
possible seven-coordinate metalloporphyrin (middle),
and eight-coordinate metalloporphyrin structure

The synthetic pathways of porphyrins have been extensively explored in the past. Over the decades, there have been multiple extraction techniques to isolate hematoporphyrin, petro porphyrins, chlorins, as well as other natural pigments abundant in nature. The isolation of these porphyrins has led researchers to synthesize synthetic porphyrins such as TPP, phthalocyanines, and a variety of macrocyclic compounds with varying substituents at the porphyrin core. These synthetic routes were explored by Rothemund, Adler and Lago, and many others, which have paved the way for researcher to synthesis, mimic, and characterize natural occurring porphyrins.

Rothemund Synthesis

One the first synthetic porphyrin, tetraphenyl porphyrin, was synthesized by Rothemund who used a condensation reaction of pyrrole and benzaldehydes with pyridine as a solvent at 150 °C for 24-48 hrs. in a sealed tube. The resulting compound was tetraphenyl porphyrin (TPP), which was recovered in low yield. The reaction was performed using severe conditions that only allowed a few substituted aldehydes to be used as reagents for conversion into the desired porphyrin.[44] Other closely related compounds such as chlorins also resulted from this synthesis which were further reduced to porphyrins by the use of 2,3-dichloro-5,6-dicyanoquinone (DDQ). Later in his career, Rothemund, successfully synthesized several meso-tetraphenyl porphyrins using different salts as he reported that his synthesis was probably the largest number of metal complex salts ever prepared from any porphyrin. The work was undertaken by Rothemund with the aim of furnishing reliable material for physio-chemical studies on the structure of porphyrin metal complexes, especially in the connection with the study of chlorophyll.[45]

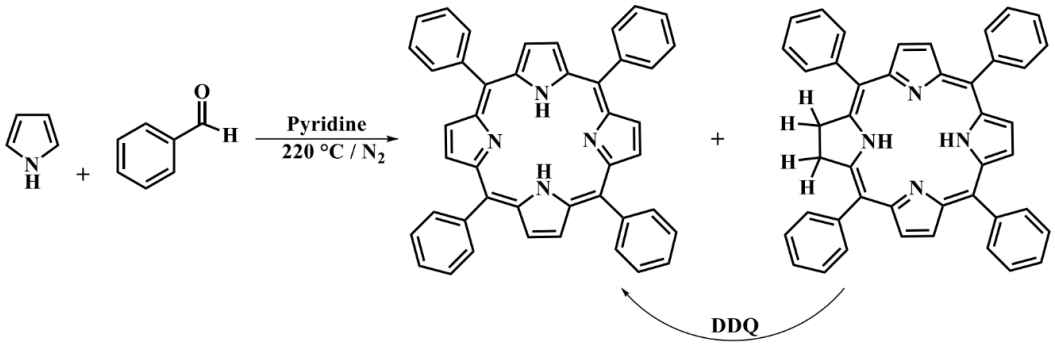

Figure 20: General Rothemund Porphyrin Synthesis

Adler-Longo Synthesis

The synthesis of porphyrins was also explored by Adler and Longo. Unlike Rothemund synthesis which required the condensation of pyrroles and aldehydes over a long time period at high temperature, with low yields, and synthesizing chlorins compound, the Adler and Longo synthesis aimed to improve and shorten reaction times and better yields. In 1964, Adler and Longo synthesized tetraphenyl porphyrin by refluxing a mixture of pyrrole and benzaldehydes in acetic acid in thirty minutes under bubbling air to oxidize all intermediates formed during the reaction. This new synthesis explored the effects of temperature, solvents, and presence of metallic salts had on the porphyrin yields.[46] Further modifying the synthesis process, Adler made improvement over the previous literature methods for synthesis of meso-tetraphenyl porphyrin. The yield and rate of the condensation of pyrrole and benzaldehyde to TPP have been found to depend on the acidity, solvent, temperature, the availability of atmospheric oxygen, and the initial concentration on the reagents which facilitated further purification for TPP.[47]However, the Adler-Longo synthesis presented two significant limitations: (1) harsh reaction conditions limits

the scope of substituents and result in complete failure with aldehydes bearing sensitive functional groups resulting in lack of any rational access to porphyrins bearing two or four distinct meso substituents and (2) the synthesis presents purification problems in many instances as well as not presenting reproducible yields.[48,49] Thus the Rothemund and Adler- Longo methods were insufficient to unlock the tremendous promise of meso-substituted porphyrins for use as building blocks in material chemistry as well as surrogates for naturally occurring porphyrins and only partially satisfied the synthesis methodology.

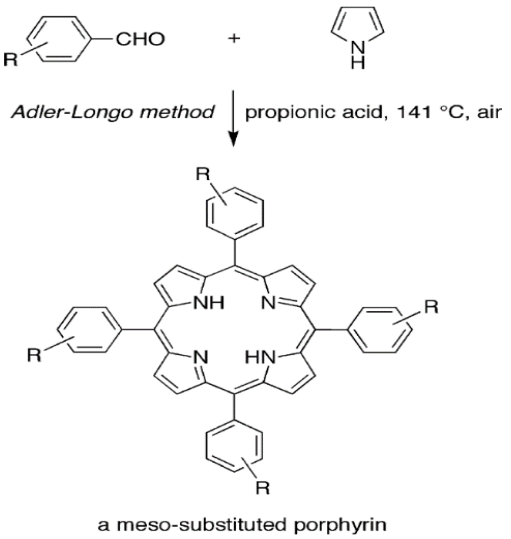

Figure 21: Adler-Longo Synthetic pathway

Lindsey Synthesis

In 1987, Jonathan S. Lindsey proposed and described a synthesis of meso-tetraphenylporphyrins[49] based on the complementary works of Rothemund and Adler and Longo which aimed at preparing small quantities of porphyrins form from sensitive aldehydes in high yield without encountering difficulty in purification procedures. Lindsey's synthesis strategy was based around studies of equilibrium cyclization and biomimetic studies of porphyrin biosynthesis and was centered around the following ideas (a) tetraphenyl porphyrinogen should

be the thermodynamically favored product when benzaldehyde and pyrrole are condensed under appropriate conditions, meaning reaction conditions that facilitate the attainment of equilibria prior to oxidation should favor high yields of porphyrin, (b) Benzaldehydes and pyrroles are reactive molecules and high temperature are not necessary for their reaction, (c) and synthetic conditions sufficiently mild for equilibrium to be achieved should also be compatible with an unprecedented variety of substituted benzaldehydes, allowing for the corresponding porphyrins to be obtained in good yields. These yields depend on the contributing factors including the choice of oxidant and acid catalyst, duration of condensation period, concentrations of acid, pyrrole, benzaldehyde, and the presence of water in the solvent. Lindsey's method only had a few drawbacks, which included several side reactions occur such as pyrrole polymerizations, non-cyclic chain formation, and combinations of aldehydes with pyrrole polymer chains which makes purification more difficult.

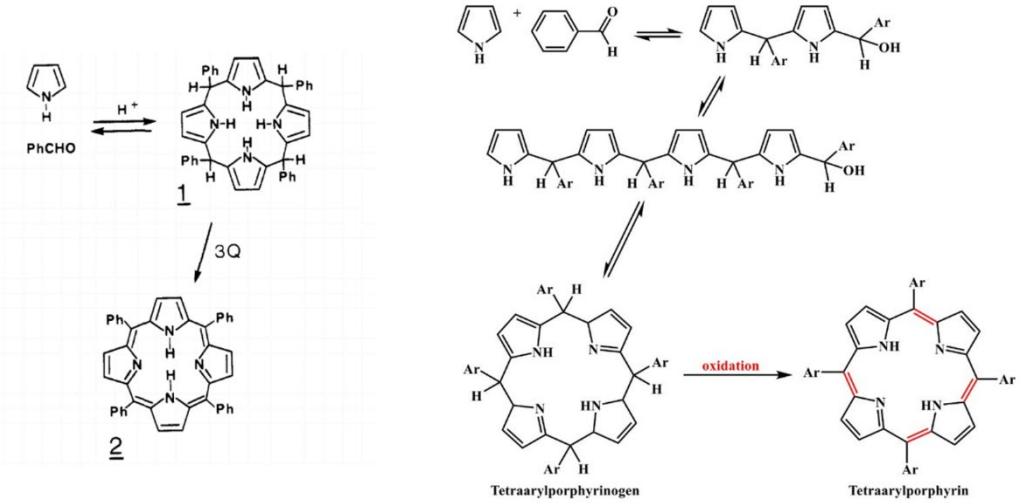

Figure 22: Lindsey's Synthetic Pathways

Microwave Activation Synthesis

Further advancing the research in porphyrin synthesis, researchers have used microwave activation techniques to improve porphyrin synthesis. Microwave assisted organic synthesis is a popular technique due to advantages such as shorter reaction times, minimum solvent requirement, and ease of purification.[50] Microwave activation applications in porphyrin synthesis include metalation and substitution of the porphyrin ligand. Microwave assisted reactions promotes the polarization of the substrate increasing the rate of the reactons.[51]Unlike the classical synthetic routes developed by Rothemund, Adler, Longo, and Lindsey that used toxic and corrosive solvents, microwave irradiation is the source of driving force for chemical reactions, making the synthesis of porphyrins and metalloporphyrins under solvent less conditions possible.[52]

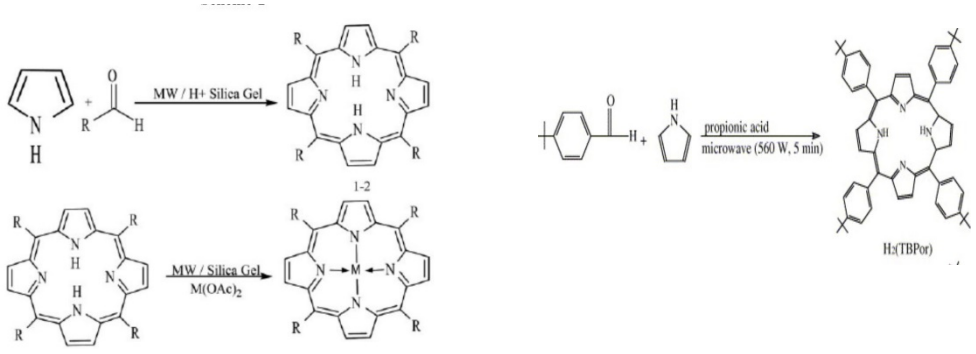

Figure 23: Examples of microwave assisted porphyrin synthesis

Porphyrin synthesis have been one of the most researched topics because of their application. Their history goes back to 1940's when Rothemund first synthesized meso-tetraphenyl porphyrin under harsh conditions. Ever since Rothemund, researchers have pioneered and established improved synthetic routes that have their own benefits and advantages. The synthetic routes previously explored here are the most relevant to this current research. The work established by researchers and their work have paved the way for scientist to keep exploring porphyrins and their derivatives. Nonetheless, there are other synthetic routes to be explored which include solid state synthesis of porphyrins, Little's synthesis, 2+2 methods, as well as many others.

CHAPTER III

MATERIALS AND METHODS

Synthesis of Tetraphenyl porphyrin:

The synthesis of the H_2TPP was performed as highlight in the literature a modified version of the Alder method were used[53,54]. In a typical synthesis benzaldehyde and pyrrole in the presence of propionic acid used. A ratio of 1:1 benzaldehyde (0.059 mol, 6mL): pyrrole (0.058 mol, 4 mL) were used with propionic acid (50 mL) as the solvent and catalysts. The reaction mixture was heated to reflux and held at reflux for 30 minutes. The reaction mixture was then cooled to room temperature. After cooling the reaction was further cooled in an ice bath. The resulting deep-purple crystals were collected by vacuum filtration and washed with cold methanol and air dried.

Synthesis of Metal Substituted Tetraphenyl porphyrin:

In a typical synthesis 0.11 g (0.18 mmol) of tetraphenyl porphyrin (H_2TPP) was reacted with 2.0 mmol of the meal chloride. The metal chlorides investigated included Ni, Cu, Co, and Pd. The metal insertion into the H_2TPP were performed using DMF and microwave assisted synthesis. The reaction was performed using reflux at 153°C for 5 minutes. A CEM Discover microwave synthesis system (C

EM Corporation Matthews, NC) was used with a 125 mL round bottom flask and a condenser. The reaction temperature was controlled by varying the microwave power and a constant readback through an infrared temperature sensor. The reaction was held a temperature for 5 minutes. After reaction the samples were cooled naturally to room temperature and filtered. The metal substituted TPP were then dried and stored. The process was repeated for all metals under investigation.

Powder X-Ray Diffraction Characterization

All four metalloporphyrin catalysts (Co TPP, Ni TPP, PdTPP, and Cu TPP) were characterized using a Bruker D2 Phaser X-Ray Diffractometer equipped with a cobalt x-ray source that emits x-rays at 1.79 Å, and a Fe filter. All the prepared samples were analyzed from a 2Θ scanning angle, 5-80° with a step size of 0.05°and 2 seconds counting time. Diffraction pattern fittings were performed using the Fullprof software and crystal structured from the literature.[55]

Fourier Transform Infrared Spectroscopy Characterizations

All four metalloporphyrin catalysts (Co TPP, Ni TPP, PdTPP, and Cu TPP) were characterized using a PerkinElmer Frontier FT-IR spectrometer. Measurements were recorded using % Intensity over the range of 4000-650 cm^{-1}.

UltraViolet-Visible Spectroscopy Characterization

All metalloporphyrin catalysts were analyzed for their ultraviolet absorption spectra using a PerkinElmer Lambda 950 UV-VIS-NIR Spectrophotometer. UV-VIS spectroscopy measurements were recorded from the power samples in % Absorption over the range of 300-700 nm.

Photochemical Catalytic reactions

Catalytic Cross-coupling and oxidations were performed with each individual catalyst. The reactions were performed in 4 mL reaction flasks under an Aldrich Micro Photochemical Reactor using a 4 W purple LED light. 10 mg of metalloporphyrin catalysts were added, 303 mg of Benzoyl Peroxide or Tert-butyl Nitrite, using either Dichloromethane, or Acetonitrile as the solvent. The oxidation reaction of aldehydes was performed in a 4mL vial under the same photochemical reactor using 2 mg of metalloporphyrin, 1.5 mmol of aromatic aldehyde substrate, 4 mL of Dichloromethane, and O_2 bubbling.

Gas Chromatography-Mass Spectrometry Studies

All samples were analyzed using Gas Chromatography-Mass Spectroscopy a Perkin Elmer Turbo Mass Gold Mass Spectrometer and a Perkin Elmer Auto system XL Gas Chromatograph were used.

CHAPTER IV

RESULTS AND DISCUSSIONS

FT-IR Analysis

Table 1: FTIR peak table and peak identification for the microwave assisted synthesized H_2TPP, CoTPP, CuTPP, NiTPP and the PdTPP compounds.

H_2TPP	CoTPP	CuTPP	NiTPP	PdTPP	Peak ID
3308.33	-	-	-	-	N-H
3053.2	3053.44	3052.61	3054.87	3051.9	C-H stretch
3021.54	3020.89	3020.44	3022.37	3021.22	
		2577.13			
1937.83	1936.3	1936.49	1937.26	1936.32	
	1874.53	1874.42	1874.89		
1796.96	1796.02	1796.88	1796.97		
	1678.88	1678.72	1675.87	1674.45	C=C
1595.59	1598.52	1597.75	1598.6	1596.72	C-C Asym
1575.12	1576.35	1576.96	1576.43	1576.9	C-C Symm
1555.8	1542.27	1534.8	1535.19	1535.13	C=C Pyrrole
1489.33	1489.3	1488.45	1489.19	1488.73	C=C Phenyl
1468.25			1460.11		-C=N-

1439.65	1439.42	1439.4	1439.16	1439.12	C-H bend pyrrole
1397.82					
	1368.06	1370.82	1376.67		
1346.77	1348.71	1344.2	1349.95	1351.4	=C-N-
	1310.5	1307.67	1312.98	1309.17	
	1241.96		1244.36		
1211.85	1206.75	1206.65	1207	1208.84	C-H Bend
1175.15	1177.54	1177.68	1177.05	1176.35	
1158.34	1159.09	1159.63	1158.8	1158.01	C-C-N
1138.41					C-C-H
1069.15	1070	1069.4	1069.92	1070.68	
1052.7					
1032.59	1033.38	1033.31			
	1022.59	1021.62	1023.17		
1001.23	1004.31	1003.47	1005.28	1012.56	
980					
965.35	963.13	963.3	963.77		In-plane bending in porphyrin
913.13	914.97	914.68	914.38		
899.63	898.39	899.4	898.99	898.09	
876.53		880.52			
838.3	833.46	832.28	833.71	833.89	Out of plane deformation of phenyl
825.94					
789.62	790.45	790.01	789.77	787.82	
723.59	739.49	739.13	740.14	740.13	
	708.36	708.96	706.64		
694.03	693.78	693.81	694.15	694.11	In plane vibration deformation of porphyrin
	682.05	681.25	682.57	680.91	
670.35	665.34	663.68	665.65	665.71	
656.06	653.33				

Infrared spectra of tetraphenyl porphyrin ligand and its metal chelates were taken and the results are shown in Table 1. One of the most notable and prominent band in the infrared spectra when comparing the TPP ligand against it metal chelates would be the weak N-H stretching vibration above 3300 cm^{-1}. This stretching vibration corresponds to a secondary amine present in the free base porphyrin ligand (TPP) and not present in the metal chelates (NiTPP, CoTPP, CuTPP, and PdTPP). The disappearance of this vibration band in the metal chelates is a strong indication of the metalation of the porphyrin ligand since the acidic hydrogens are replaced by the metal ion. Replacement of these hydrogen atoms results in shifts of many absorption bands of the ligand to both higher and lower frequencies. These shifts to higher frequency are more pronounced in three sharp absorption bands for tetraphenyl porphyrin ligand near the 960, 980, and 1000 cm^{-1}. The strong absorption band near 1000 cm^{-1}appears to be a vibration characteristic of all the tetraphenyl porphyrin chelates, and the frequency of the band varies with the nature of the meatal ion. Furthermore, the band may be associated with a rocking vibration of the porphyrin ring or the pyrrole units, which is sensitive to the nature of the metal ions and which is related to the strength of the metal-nitrogen bonds in the tetraphenyl metalloporphyrin. Table 1 shows the results and further supports this statement by either showing the metalloporphyrins having lower or higher frequencies as well as comparing the infrared spectrums and values to the existing literature.[62,63]

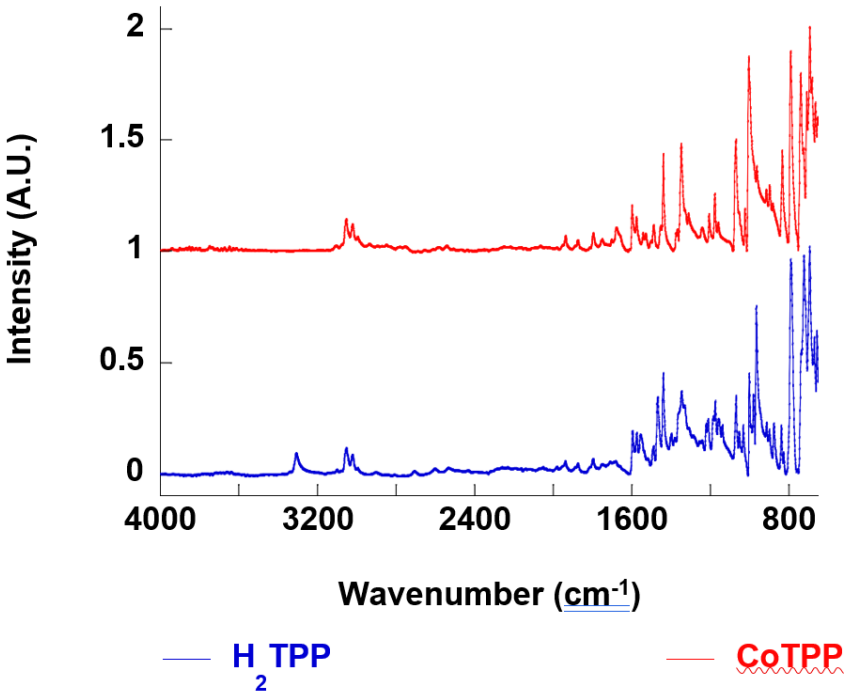

Figure 24: FTIR of the H_2TPP and CoTPP compounds synthesized under microwave assisted conditions.

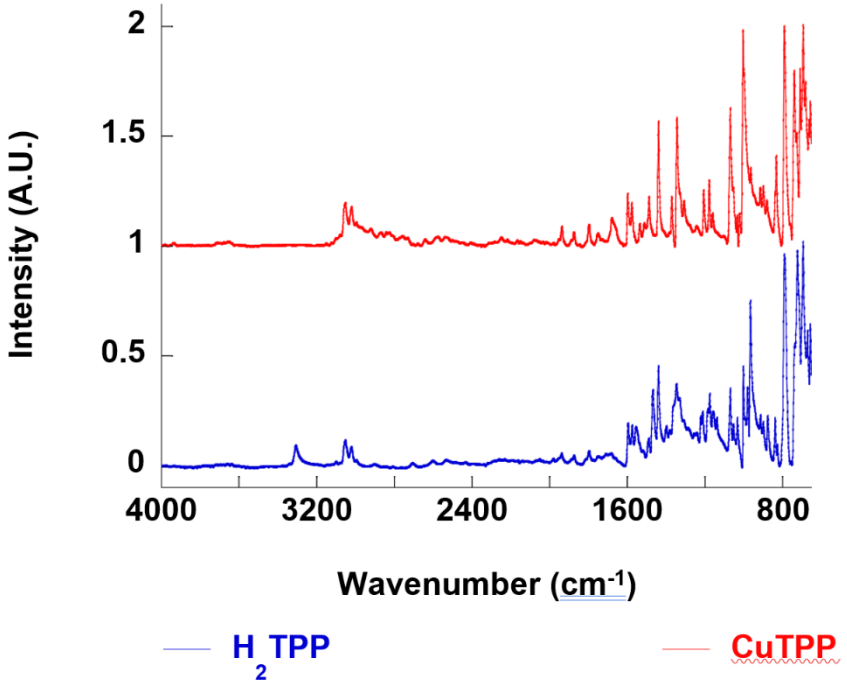

Figure 25: FTIR of the H_2TPP and CuTPP compounds synthesized under microwave assisted conditions.

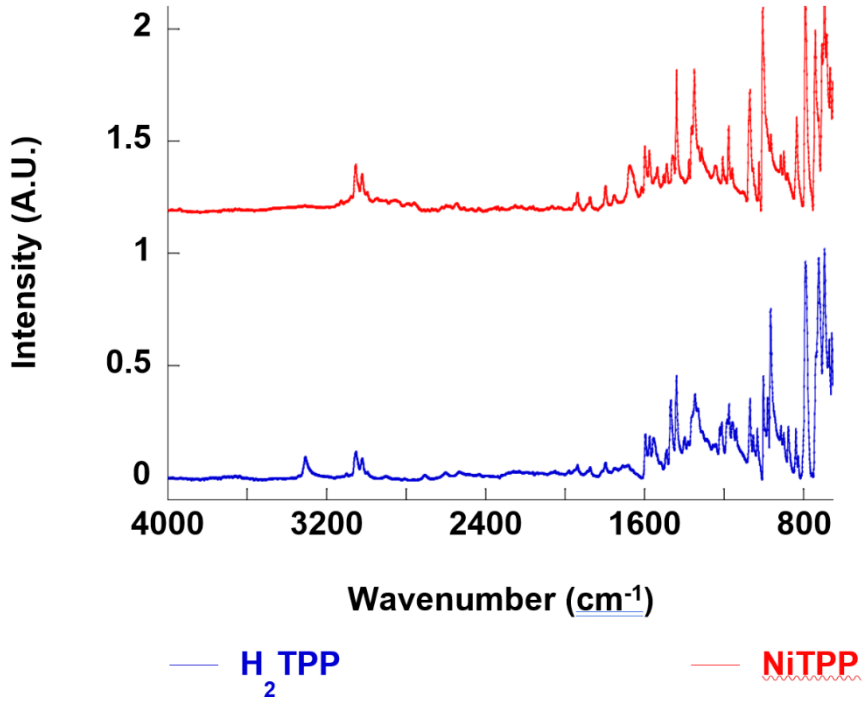

Figure 26: FTIR of the H_2TPP and NiTPP compounds synthesized under microwave assisted conditions.

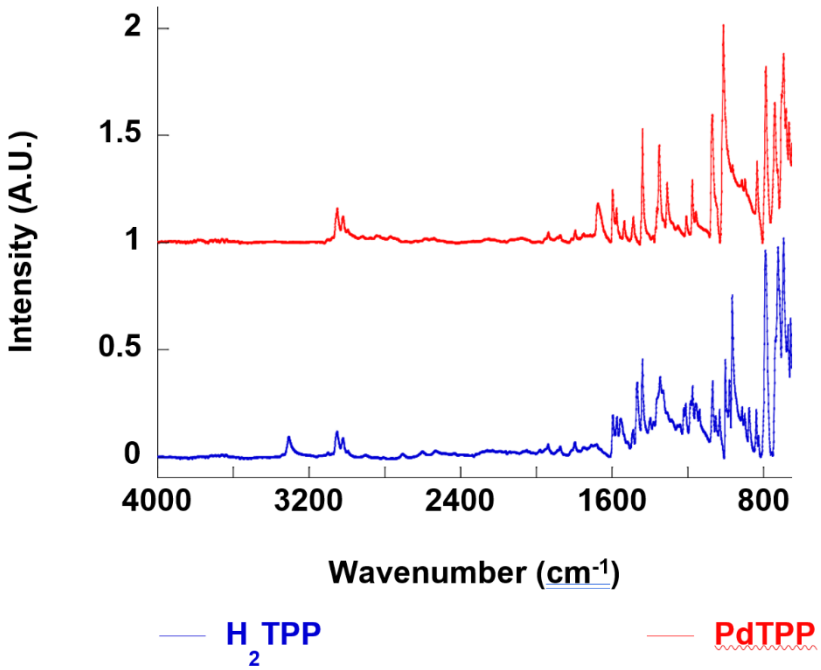

Figure 27: FTIR of the H_2TPP and PdTPP compounds synthesized under microwave assisted conditions.

X-Ray Diffraction Analysis

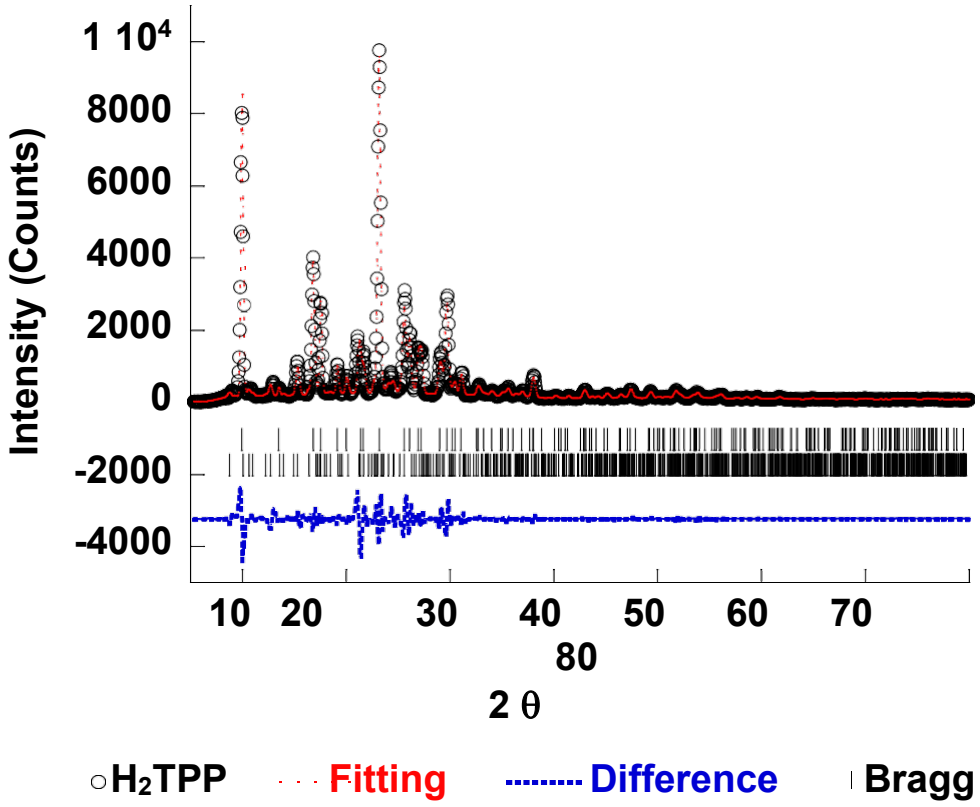

Figure 28: Powder X-ray diffraction of the H_2TPP compound synthesized under microwave assisted conditions.

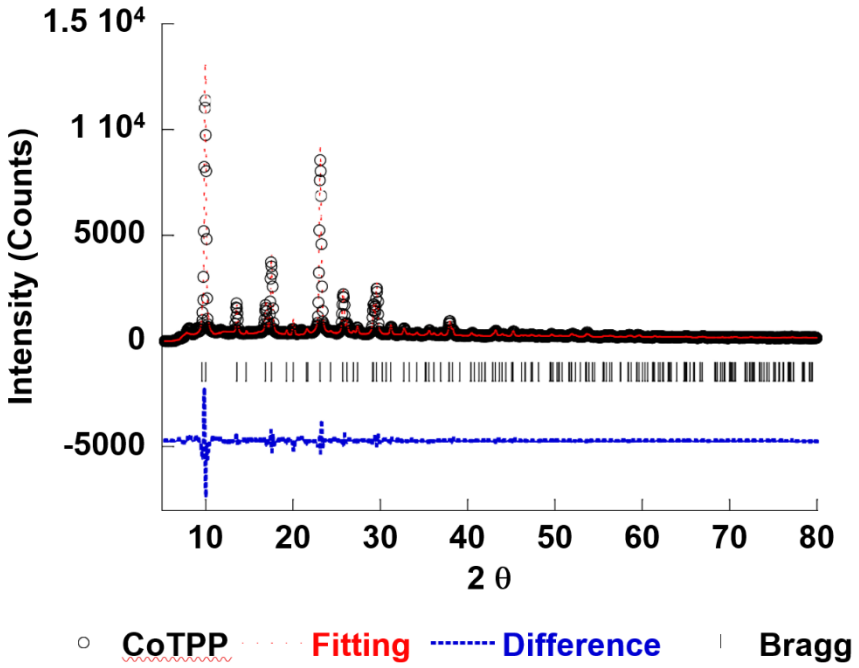

Figure 29: Powder X-ray diffraction of the CoTPP compound synthesized under microwave assisted conditions.

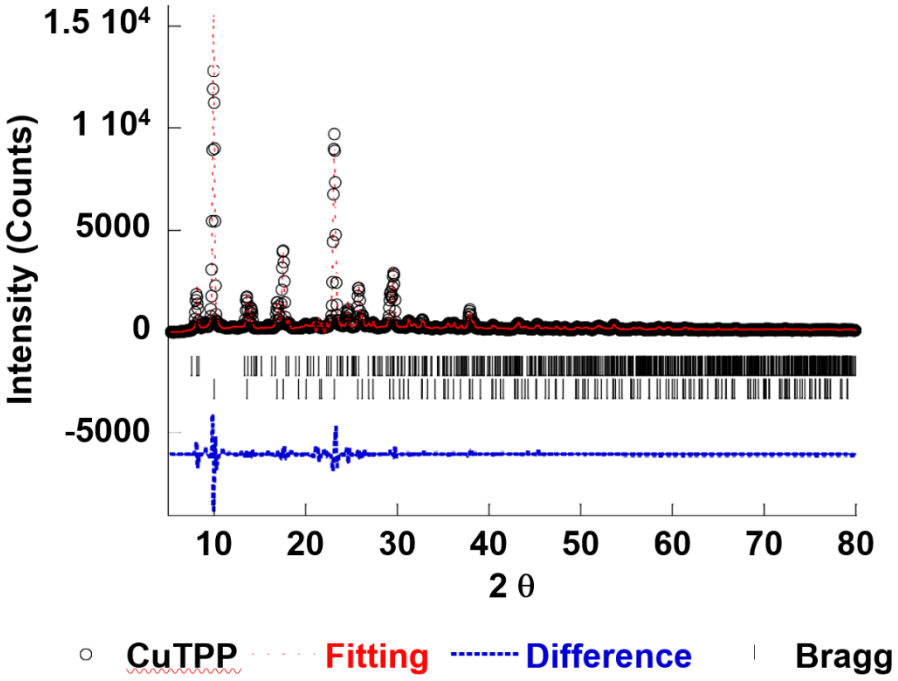

Figure 30: Powder X-ray diffraction of the Cu TPP compound synthesized under microwave assisted conditions.

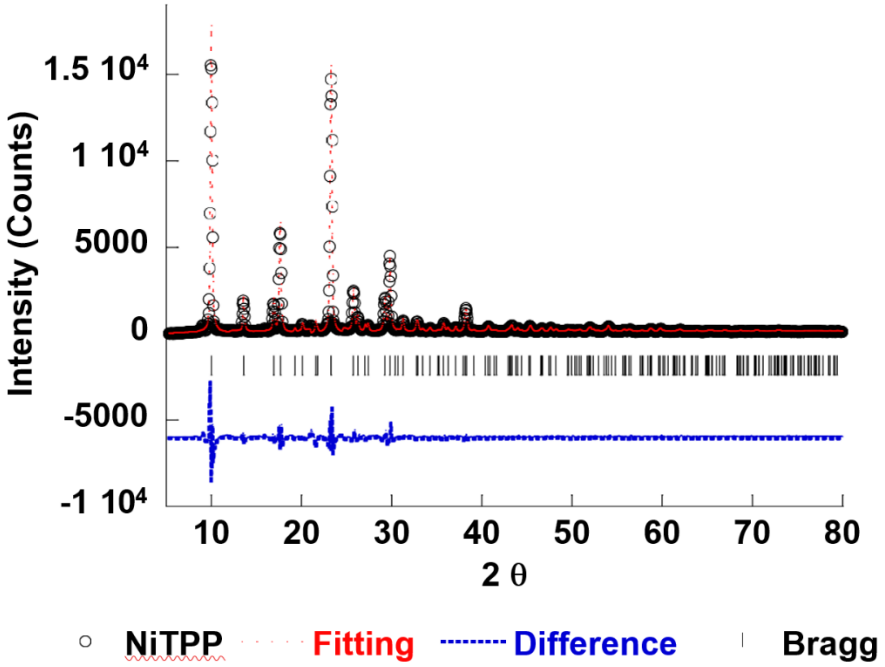

Figure 31: Powder X-ray diffraction of the NiTPP compound synthesized under microwave assisted conditions.

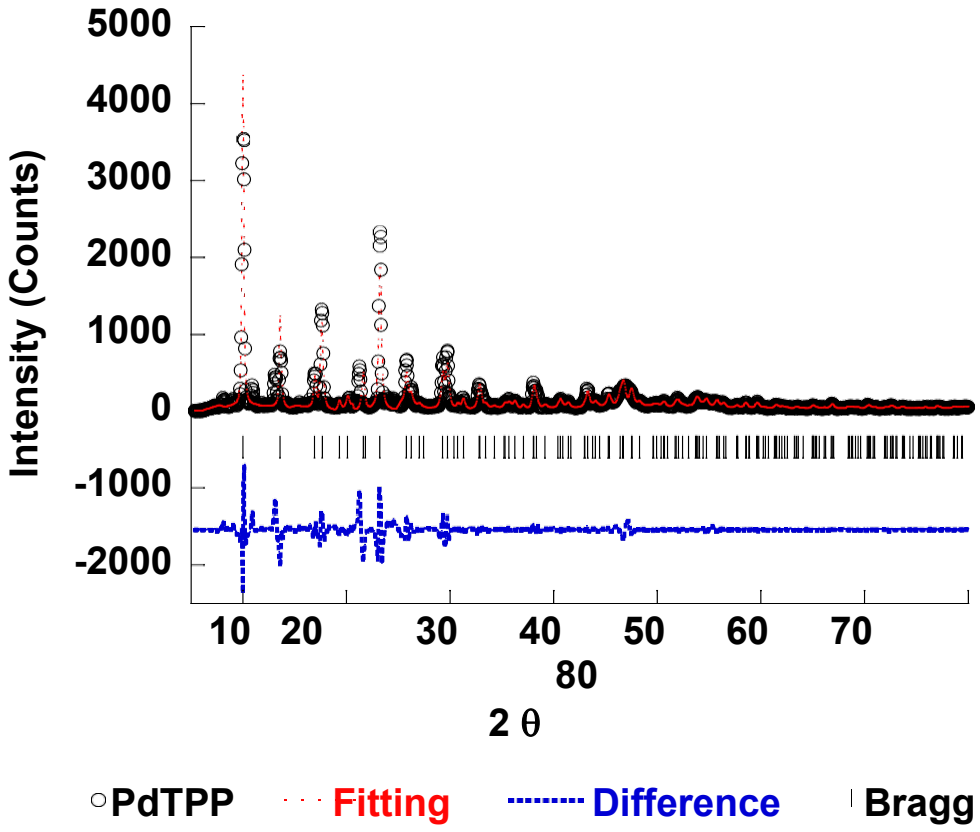

Figure 32: Powder X-ray diffraction of the PdTPP compound synthesized under microwave assisted conditions.

Table 2: Fullprof fitting results for the H_2TPP, CoTPP, CuTPP, NiTPP and PdTPP microwave assisted synthesized compounds

Sample	Space Group	a(Å)	b(Å)	c(Å)	α(°)	β(°)	γ(°)	GOF
H_2TPP	I-42/d	15.203(6)	15.203(6)	13.955(8)	90.00	90.00	90.00	4.1
	P212121	12.022(5)	19.308(5)	14.695(4)	90.00	90.00	90.00	
CoTPP	I-42/d	15.086(2)	15.086(2)	13.988(6)	90.00	90.00	90.00	3.2
CuTPP	P21/M	15.091(8)	8.646(1)	12.004(4)	90.00	116.02	90.00	3.5
	I-42/d	15.106(4)	15.106(4)	13.996(2)	90.00	90.00	90.00	
NiTPP	I-42/d	15.093(0)	15.093(0)	13.891(8)	90.00	90.00	90.00	4.3
PdTPP	I-42/d	15.062(1)	15.062(1)	13.916(1)	90.00	90.00	90.00	4.4

Note: GOF (goodness of fit) a value of less than 5 is a suitable fitting value.

Fitted diffraction patterns for all synthesized metalloporphyrin catalysts are shown in Figures 28-32. The circular dots indicate the diffraction pattern for a given sample while the red dashed line indicates the diffraction fitting. The blue dashed line indicates the difference between the diffraction pattern for the sample and the diffraction fitting, and the vertical lines or markings indicate the Braggs planes. From the results on Table 2, the free porphyrin ligand H_2TPP has two space groups I-42/d and P212121, indicting the porphyrin was present in 2 phases in tetragonal and orthorhombic crystal lattices, respectively. The I-42d space group is present in all the synthesized porphyrin catalysts making them adopt a tetragonal crystal structure. CuTPP has two space groups I-42d and P21/M, showing the presence of both tetragonal and monoclinic crystals. The space groups, phases, and parameters in the materials were consistent with the literature values.[55] The average parameters for each catalyst is summarized on table 2. In H_2TPP for space

group I-42d, a = b = 15.20 Å and c = 13.96; for space group P212121 a = 12.02, b = 19.31, c = 14.69. For CoTPP, CuTPP, NiTPP, and PdTPP which share the same I-42d space group, a = b = 15.10 and c = 13.90. CuTPP also has a P21/M space group with parameters, a = 15.10, b = 8.65, and c = 12.00. The angles α, β, ϒ for the metalloporphyrins in space group I-42/d and P212121 are 90˚, 90˚, and 90˚, respectively. The angles α, β, ϒ for space group P21/M is CuTPP are 90˚, 116˚, and 90˚, respectively. All fittings show a good agreement between the collected data and the literature values, which show χ^2 (goodness of fit value) values below 5.

UV-Vis Analysis

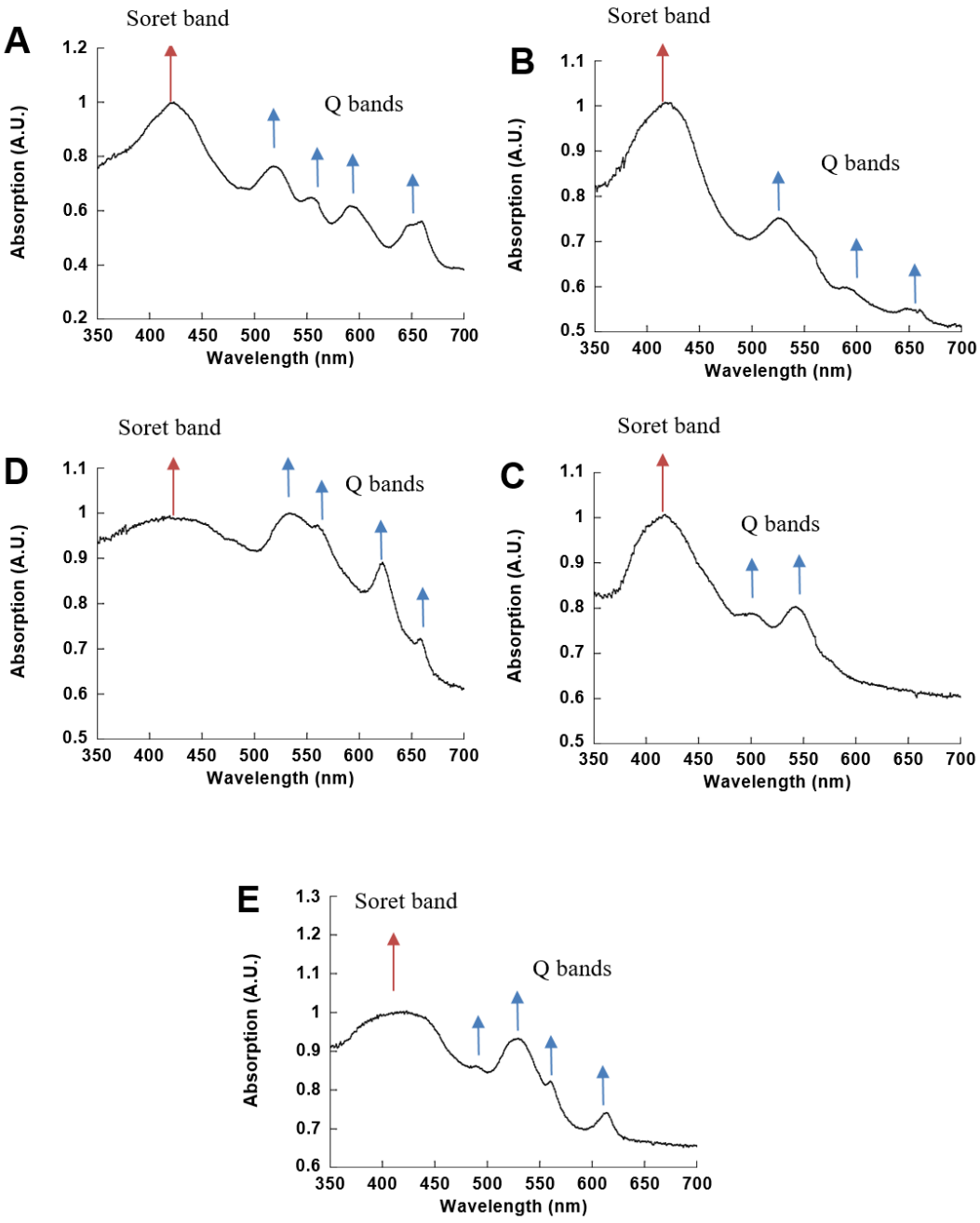

Figure 33: UV-Vis spectrum for the A.) H_2TPP, B.) CoTPP, C.) CuTPP D.) NiTPP, and E.) PdTPP samples as synthesized.

Table 3: Identified peaks in the UV-Vis spectrum for the H_2TPP, CoTPP, CuTPP, NiTPP, and PdTPP samples as synthesized.

Sample	Peak location (nm)	Absorption Band
H_2TPP	421	Soret (B)
	518	Q
	556	Q
	594	Q
	654	Q
CoTPP	420	Soret (B)
	525	Q
	593	Q
	652	Q
CuTPP	418	Soret (B)
	503	Q
	543	Q
NiTPP	425	Soret (B)
	532	Q
	560	Q
	622	Q
	658	Q
PdTPP	420	Soret (B)
	489	Q
	528	Q
	561	Q
	612	Q

Porphyrin compounds absorbs visible light and convert photo-energy to electric energy. The porphyrin skeleton has an extended π-conjugation system with a 24-π electron system that leads to a wide range of wavelengths for light absorption. The absorption spectra of the porphyrin compounds are well known, and their bands in different regions are denoted as Q, B, N, L and M.[56] The most notable absorption bands present in the porphyrin compounds are the Q bands, weak absorption in the visible region, and Soret bands, B, are the more intense absorption bands near the ultraviolet region. The Soret (B) band consists of a strong transition to the second excited state, ($S_0 \rightarrow S_2$); on the other hand, the Q bands consists of weak

transitions to the first excited state ($S_0 \rightarrow S1$). The B and Q bands arise from π-π* transitions and are justified through HOMO and LUMO frontier orbitals (Gouterman Four Orbital Model) . The N, L, and M bands are also weak absorptions bands in the ultraviolet region. There are two visible bands: Q(0,0) which represents excitation from the lowest vibrational of the ground state-singlet to the lowest vibrational level of the first excited singlet electronic state, and Q(1,0) which has one quantum of vibration in the first excited singlet electronic state. [57] The Q and B bands arise form a linear combination of the one-electron transitions. For the lower Q band, the transition dipoles nearly cancel giving rise to the relatively weak absorptions in the visible region. For the higher energy B band, the transition dipoles reinforce, resulting in the very intense absorption in the UV region.[58] The Gouterman model (HOMO_1, HOMO, LUMO, LUMO $_{+1}$) demonstrate that absorption bands in a porphyrin system arise from a transition of the two HOMOs and the two LUMOs. The HOMOs were calculated to be nearly degenerate in the a_{1u} and a_{2u} orbitals while the LUMOs were calculated to be a degenerate set of the e_g orbitals. Transitions between these orbitals gave rise to two excited states, both of ^1E_u character. Orbital mixing splits these two states in energy by configuration interaction into two pairs of degenerate orbitals, creating a higher energy ^1E_u as shown in figure 34.[59]

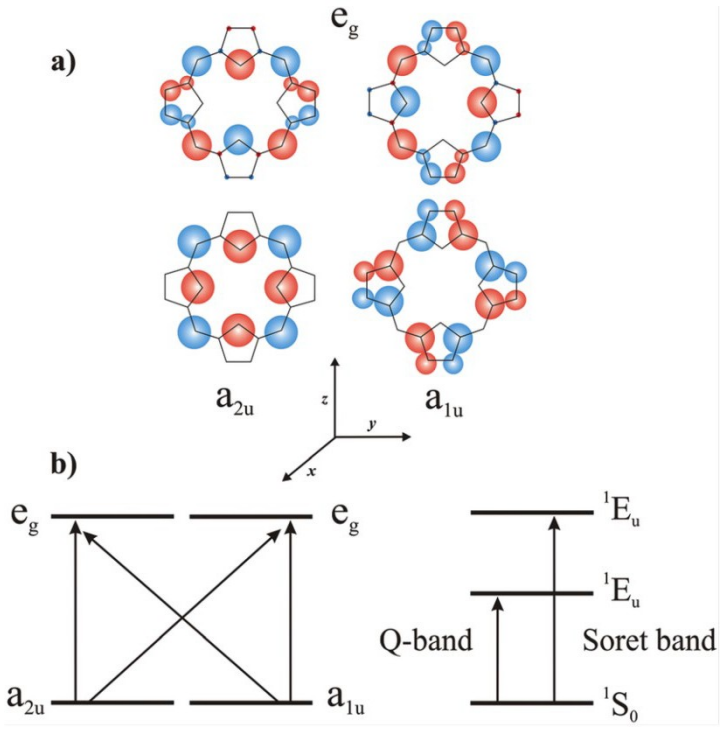

Figure 34: a) Gouterman's four orbital model (HOMO/LUMO b) energy levels showing the transitions of a porphyrin system

Figure 33 represents the UV-Vis spectrum of the porphyrin ligand as well as the synthesized metalloporphyrins. The absorbance range was recorded for each sample was form 350-700 nm, where the Q and Soret (B) bands are present in the compound. Spectra A shows the parent ligand tetraphenyl porphyrin (H2TPP) having absorption bands at 421, 518, 556, 594, and 654. H_2TPP spectra clearly showed Soret band in the blue region (400-550 nm) which include one intense band at 421 nm. [60] This intense band is the product of the excitation of H_2TPP compound which also displayed the smaller Q bands in the region (500-650) which includes four less intense bands at 518 nm, 556 nm, 594 nm, and 654 nm. Spectra B corresponds to the metalloporphyrin CoTPP and it has four absorption bands 420 nm, 525 nm, 593 nm, and 652 nm. CoTPP has a Soret band at 420 and it only slightly shifted 1 nm compared to the free base

porphyrin, H_2TPP. CoTPP also shows 3 absorption bands belonging to the Q band region; The bands at 525 nm, 593 nm, and 652 nm also shifted from their original position in the parent compound. The band in H2TPP at 556 nm was not present in CoTPP, confirming the metalation by addition of the Cobalt metal center in the free base porphyrin. Spectra C corresponds to CuTPP and has a Soret band that slightly shifted at 418 nm and has two less absorption bands in the Q region, displaying only the shifted bands 503 nm and 543 nm, when compared to the original compound H2TPP. Spectra D and E, NiTPP and PdTPP, respectively, displayed shifted absorption bands. NiTPP has a broad, intense Soret band at 425 nm, along with four absorption bands representing the Q bands at 532 nm, 560 nm, 622 nm, and 658 nm. PdTPP broad Soret band is identified at 420 nm. The Q absorption bands can be located at 489 nm, 528 nm, 561 nm, and 612 nm. The shift and intensity of the bands is contributed to the metalation of the free porphyrin base, H_2TPP. Different metal functionalization affects the absorption bands intensities, positions, and may remove them completely.

To further understand the spectroscopic shifts of the free base tetraphenyl porphyrin and metal substituted tetraphenyl porphyrin, Marsh and Mink[61] describes the effect of the metal has on the absorption spectra of tetraphenyl porphyrin. As previously mentioned, the absorption bands in the porphyrin system arise from the transitions between two HOMO and two LUMO, and it is the identities of the metal center and the substituents on the ring that affect the relative energies of the transitions. Metalloporphyrins can be divided into two groups based on their UV-VIS and fluorescence properties, Regular and Hypsoporphyrins. Regular metalloporphyrins contain closed shell metal ions (d^0 or d^{10}), e.g., Zn (II) in which the $d\pi$ (d_{XZ}, d_{XY}) metal-based orbitals are relatively low in energy, having very little effect on the porphyrin π to π^* energy gap in porphyrin electronic spectra. On the other hand, Hypsoporphyrins are metalloporphyrins in

which the metals are of d^m, where m = 6-9 and having filled dπ orbitals. In these Hypsoporphyrins- types of metalloporphyrins, there is a considerable metal dπ to porphyrin π^* orbital interaction (metal to ligand π-back bonding). Resulting in an increased porphyrin π to π^* energy separation causing the electronic absorption to undergo hypsochromic (blue) shifts.

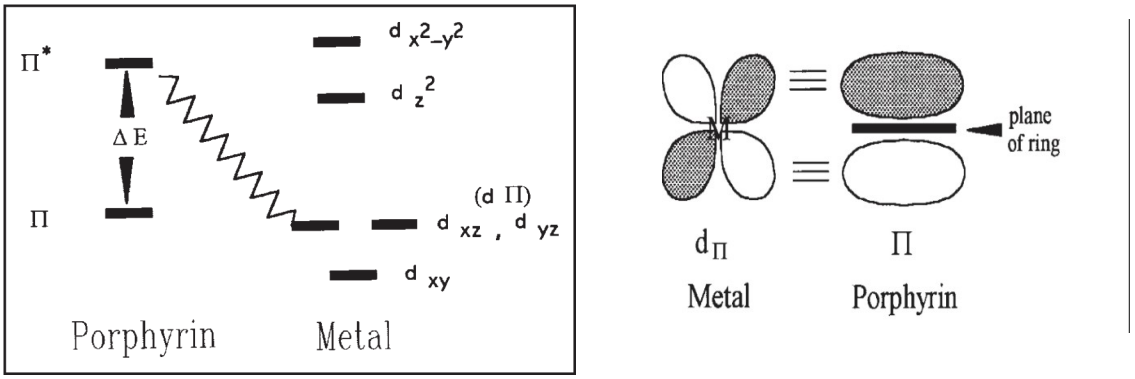

Figure 35: Porphyrin-Metal Molecular Diagram interaction (left) and Porphyrin-Metal π orbital interactions (right)

The shifts in the metalloporphyrin to shorter wavelength is due to the metal dπ (d_{xz} and d_{xy}) to porphyrin π^* back bonding as shown in Figure 35. The back bonding raises the porphyrin π^* orbitals to higher energy, resulting in an increase of ΔE and a decrease in fluorescent yield. The change in the spectrum such as fewer bands on the metalation is due to an increase of symmetry relative to the free base porphyrin ligand. The two hydrogens in the pyrrole nitrogen atoms (NH) in the porphyrin ligand reduces the ring symmetry from square planar (D_{4h}) in metalloporphyrins to rectangular (D_{2h}) in free base porphyrin.

Photocatalytic Reactions Analysis

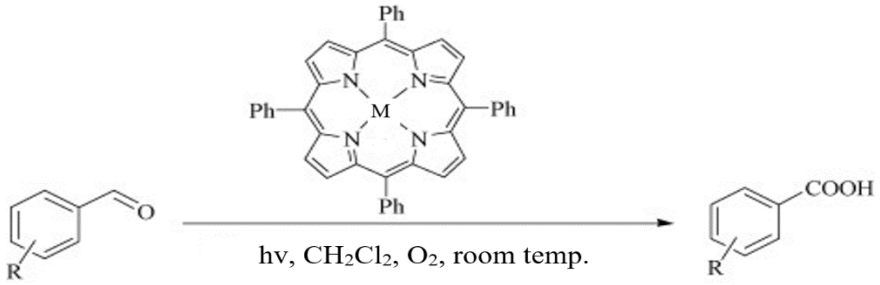

Figure 36: Photocatalytic Metalloporphyrin oxidation of aldehydes to corresponding carboxylic acids

Table 4: Compounds identified in the reaction of Trans-cinnamaldehyde (TCAlde) with propanaldehyde (PAld) in dichloromethane (DCM) in the presence of CoTPP, CuTPP, NiTPP, and PdTPP.

CO TCAld PAld DCM

Compound	Peak number	RT
2,6-diethyl-5-methyl-[1,3]dioxan-4-ol	1	3.53
1-Pentanol	2	3.77
5-Methyl-2-heptanol	3	3.95
3-Methylbenzoic acid	4	4.11
Propanoic Acid	5	4.79
Glyceryl diacetate 1-linolenate	6	7.05
Glyceryl diacetate 2-oleate	7	7.29
diacetyl glyceryl oleate	8	7.46
Glyceryl diacetate 2-oleate	9	7.62
diacetyl glyceryl oleate	10	7.74
9-Octadecenoic acid (Z)-, 2,3-bis(acetyloxy)propyl ester	11	7.95
9-Octadecenoic acid (Z)-, 2-(acetyloxy)-1-((acetyloxy)methyl)ethyl ester	12	8.05

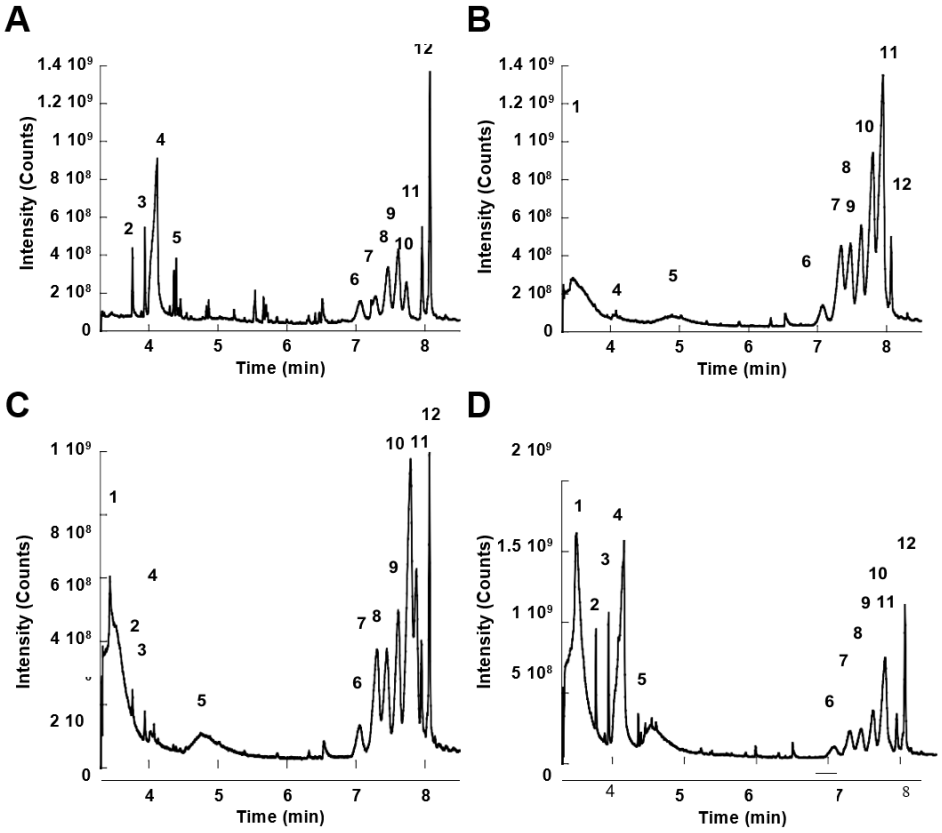

Figure 37: GC-MS plots of the reaction of TCAld with PAld in DCM as the solvent A.) CoTPP, B.) CuTPP, C.) NiTPP, and D.) PdTPP

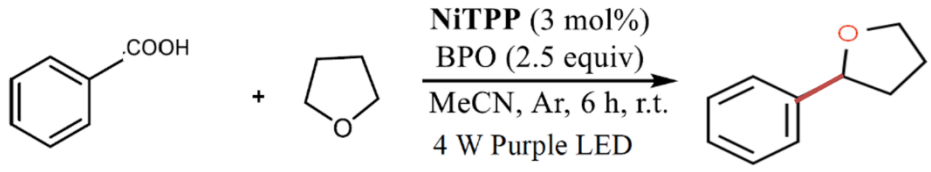

Figure 38: Metalloporphyrin reaction in the presence of benzoic acid, tetrahydrofuran, and benzoyl peroxide in acetonitrile under light irradiation

Table 5: Compound identified in the mass spectrum for the reaction of Benzoyl peroxide (BPO) with Benzoic Acid (BA) and Tetrahydrofuran (THF) in Acetonitrile (MeCN) in the presence of CoTPP, CuTPP, NiTPP, and PdTPP.

Sample	Compound	Peak number	RT
BA BPO THF MeCN	Benzoic Acid	1	4.14
	Biphenyl	2	4.52
	2-phenyloxolane	3	5.48
	Benzoic acid phenyl ester	4	5.97
	Biphenyl-2-carboxylic acid	5	6.58
	terphenyl	6	6.95
	Biphenyl-4-carboxylic acid	7	7.12
	4-Hydroxy-9-fluorenone	8	7.49

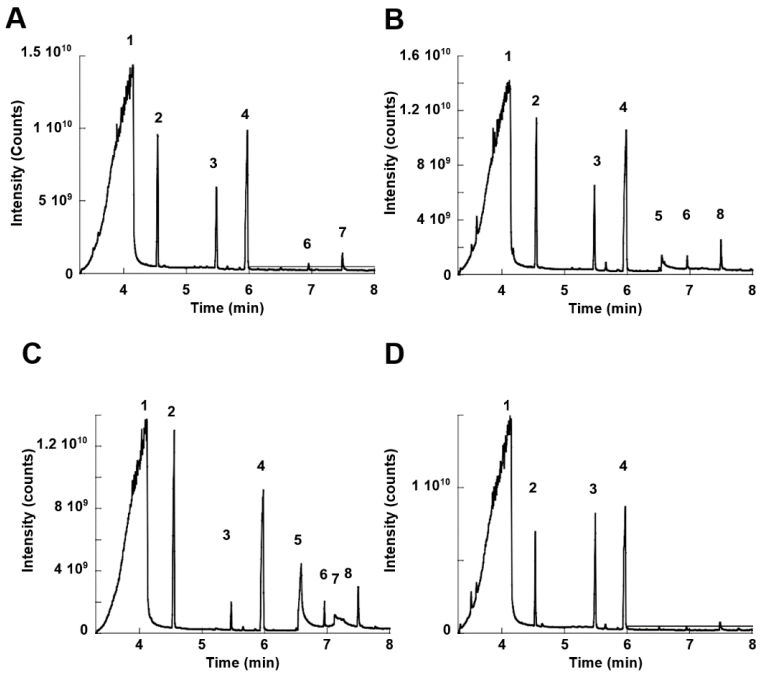

Figure 39: GC-MS plots of the reaction of BPO with THF in MeCN as the solvent A.) CoTPP, B.) CuTPP, C.) NiTPP, and D.) PdTPP

Co BPO Ba THF MeCN No Reaction Peak is benzoic acid

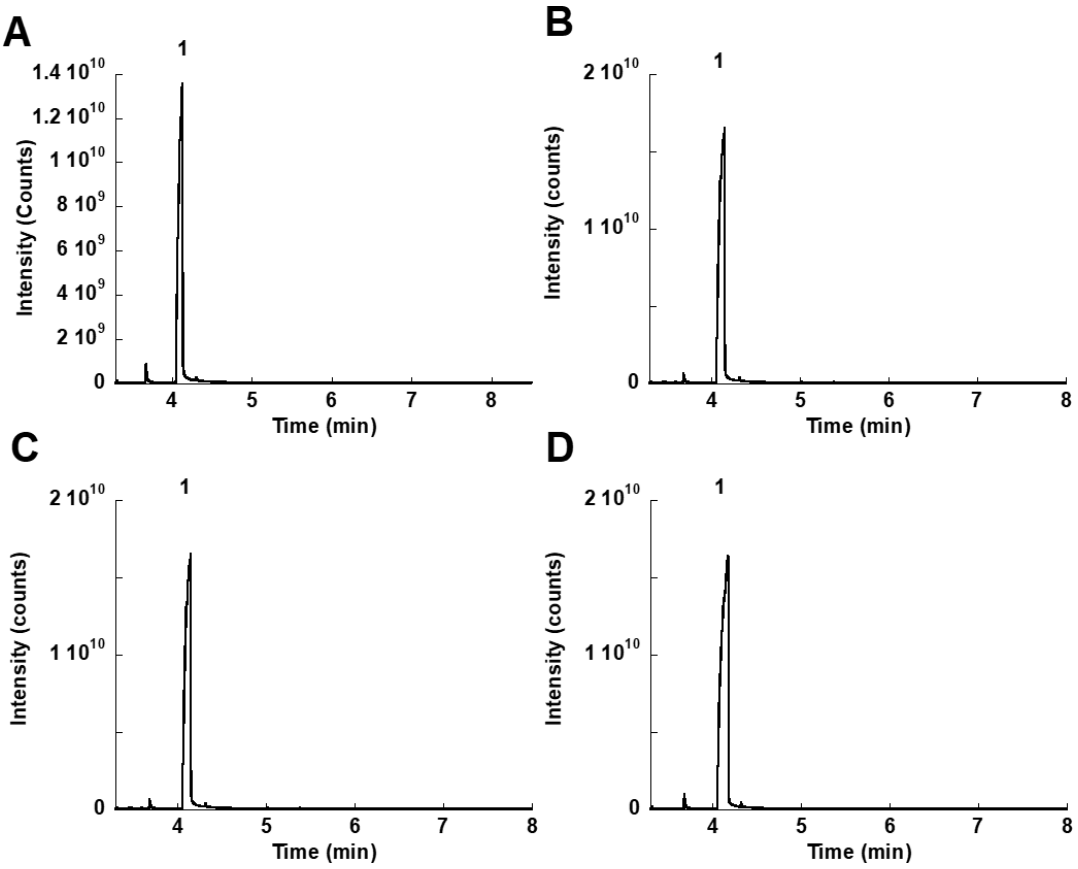

Figure 40: GC-MS plots of the reaction of BPO BA with THF in MeCN as the solvent A.) CoTPP, B.) CuTPP, C.) NiTPP, and D.) PdTPP

BA THF No reaction peak is benzoic acid

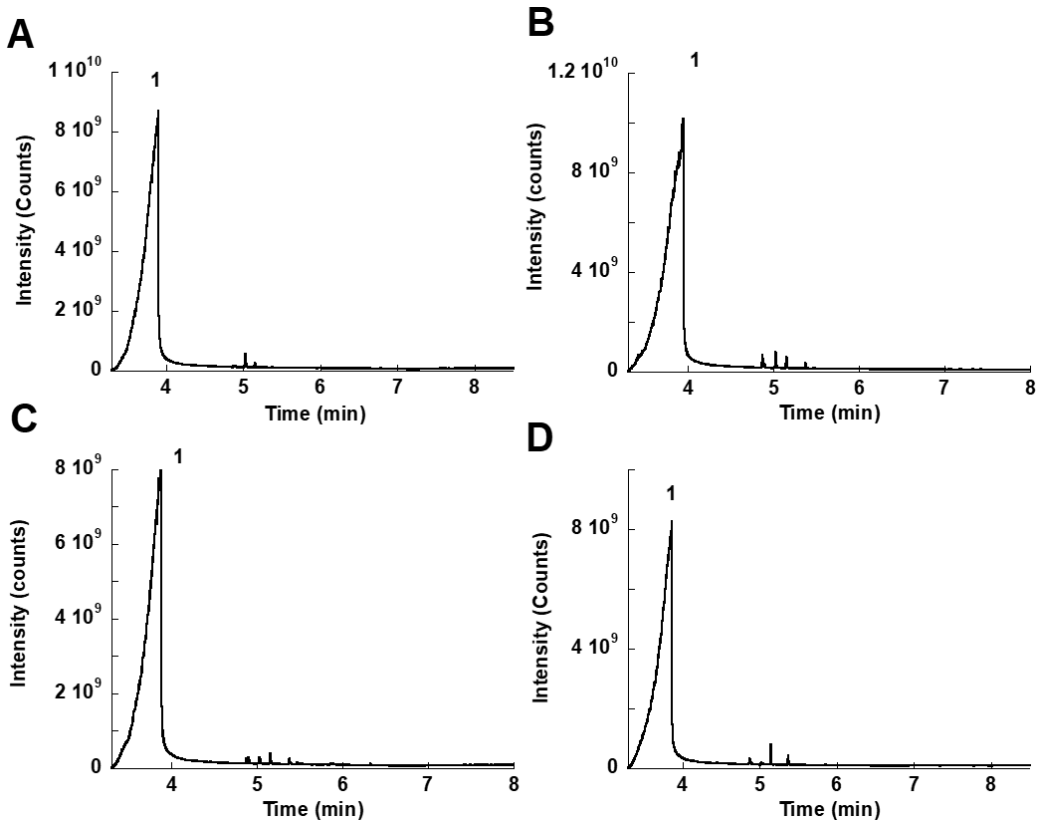

Figure 41: GC-MS plots of the reaction of BA THF as solvent A.) CoTPP, B.) CuTPP, C.) NiTPP, and D.) PdTPP

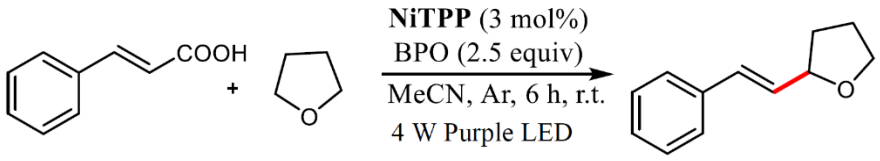

Figure 42: Metalloporphyrin reaction in the presence of trans-cinnamic acid, tetrahydrofuran, and benzoyl peroxide in acetonitrile under light irradiation

Table 6: Compound identified in the mass spectrum for the reaction of BPO THF with Trans-Cinnamic Acid (TCA) in Acetonitrile in the presence of CoTPP, CuTPP, NiTPP, and PdTPP.

Sample	Compound	Peak number	Retention Time
TCA BPO THF MeCN	Benzoic Acid	1	3.67
	Biphenyl	2	4.52
	Cinnamic Acid	3	4.99
	Benzene phenyl ester	4	5.92
	stilbene	5	6.21
	phenyl 3-phenylpropanoate	6	6.99
	phenyl 3-phenylpropanoate	7	7.33

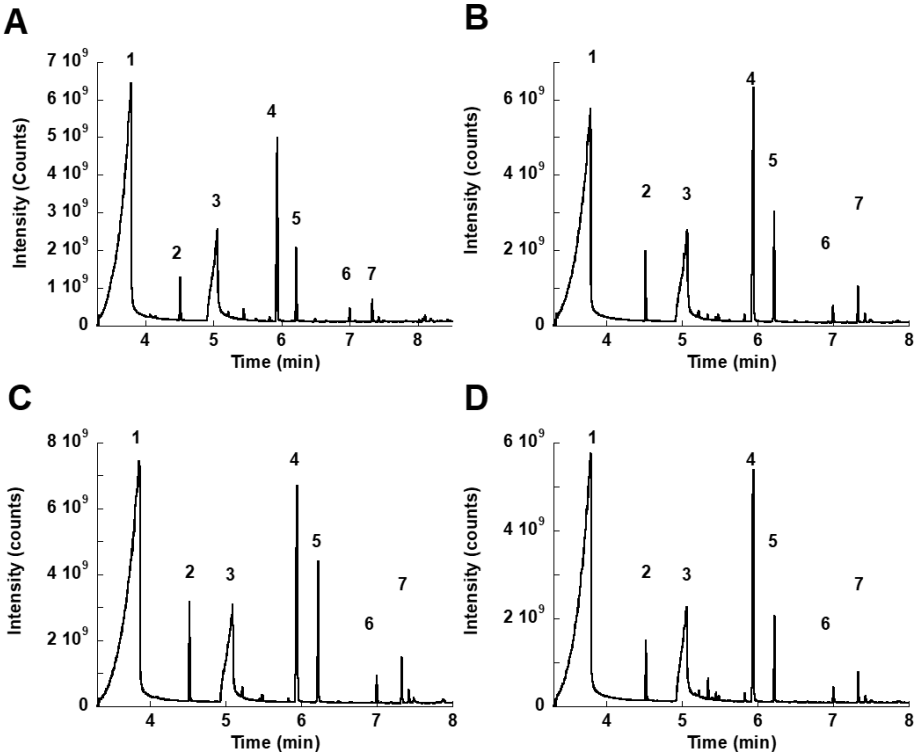

Figure 43: GC-MS plots of the reaction of BPO THF with TCA in acetonitrile A.) CoTPP, B.) CuTPP, C.) NiTPP, and D.) PdTPP

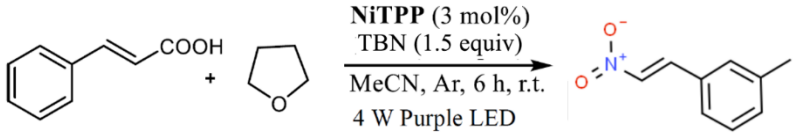

Figure 44: Metalloporphyrin reaction in the presence of trans-cinnamic acid, tetrahydrofuran, tert-butyl nitrite in acetonitrile under light irradiation

Table 7: Compound identified in the mass spectrum for the reaction of tert-butyl nitrite (TBN) with TCA and THF in with in acetonitrile in the presence of CoTPP, CuTPP, NiTPP, and PdTPP.

Sample	Compound	Peak Number	Retention Time
Co TBN THF TCA MeCN	THF	1	3.51
	Styrene 2-nitroethylene	2	4.82
	Cinnamic Acid	3	5.15

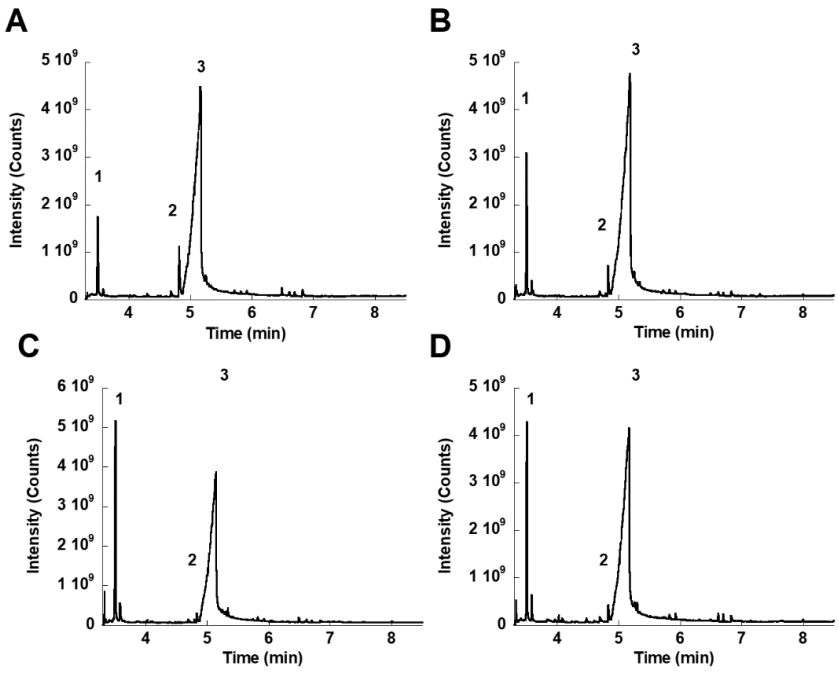

Figure 45: GC-MS plots of the reaction of CA with TBN in and THF in MeCN as the solvent A.) CoTPP, B.) CuTPP, C.) NiTPP, and D.) PdTPP.

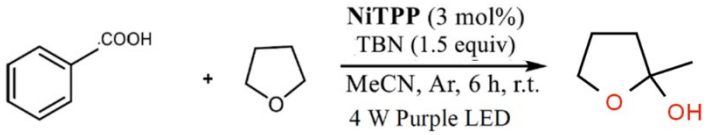

Figure 46: Metalloporphyrin reaction in the presence of benzoic acid, tetrahydrofuran, tert-butyl nitrite in acetonitrile under light irradiation

Table 8: Compound identified in the mass spectrum for the reaction of TBN with BA and THF in with in acetonitrile in the presence of CoTPP, CuTPP, NiTPP, and PdTPP.

Sample	Compound	Peak Number	Retention Time
TBN THF BA MeCN	tetrahydro-2-methyl-2-furanol	1	3.51
	benzoic acid	2	3.76

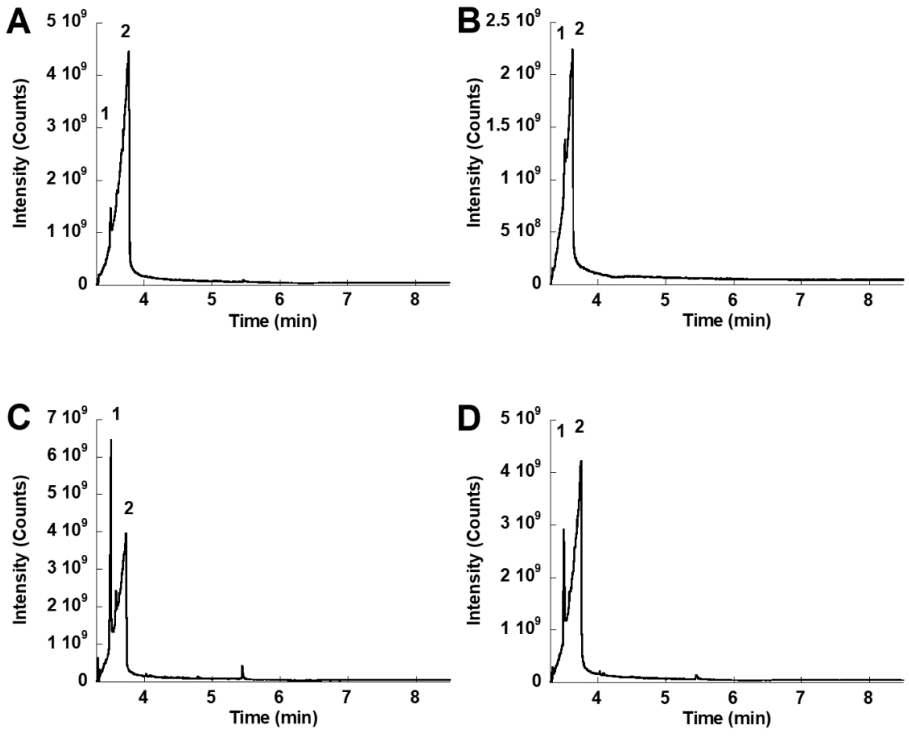

Figure 47: GC-MS plots of the reaction of BA with TBN in and THF in MeCN as the solvent A.) CoTPP, B.) CuTPP, C.) NiTPP, and D.) PdTPP.

Table 9: Compound identified in the mass spectrum for the reaction of TCA with air in DCM as the solvent in the presence of CoTPP, CuTPP, NiTPP, and PdTPP.

Sample	Compound	Peak Number	Retention Time
	3-Methylbenzoic acid	1	4.03
	Glyceryl diacetate 2-oleate	2	6.91
	Glyceryl diacetate 1-linolenate	3	7.05
	Glyceryl diacetate 2-oleate	4	7.29
	diacetyl glyceryl oleate	5	7.46
	Glyceryl diacetate 2-oleate	6	7.62
	diacetyl glyceryl oleate	7	7.74
	9-Octadecenoic acid (Z)-, 2,3-bis(acetyloxy)propyl ester	8	7.95
	9-Octadecenoic acid (Z)-, 2- (acetyloxy)-1-((acetyloxy)methyl)ethyl ester	9	8.05

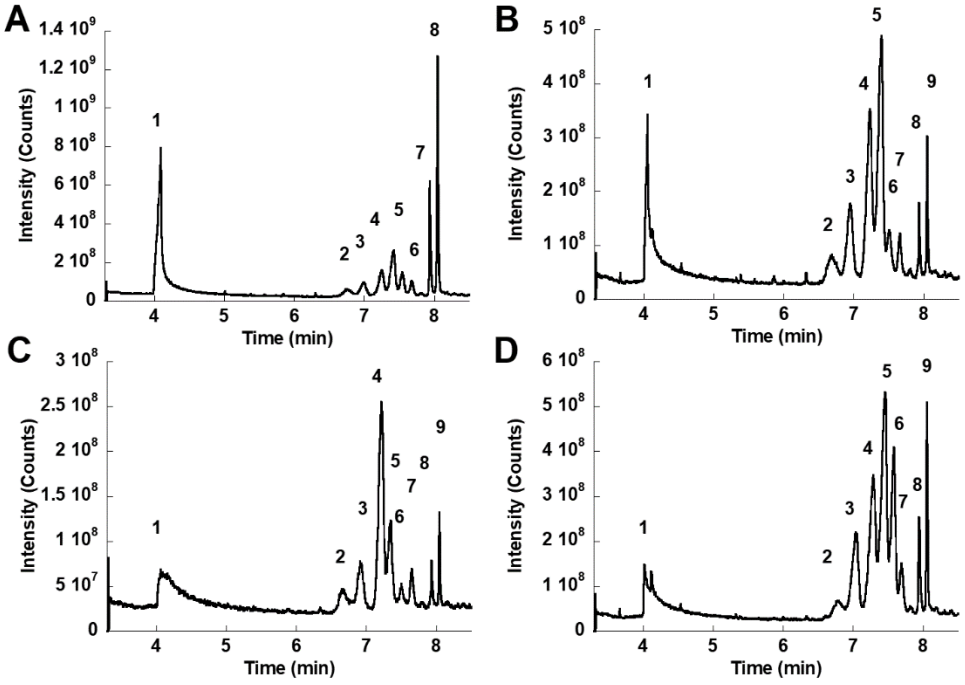

Figure 48**:** GC-MS plots of the reaction of TCA with air in DCM as the solvent A.) CoTPP, B.) CuTPP, C.) NiTPP, and D.) PdTPP .

GC-MS analysis for the possible photocatalytic reactions revealed the performance and products of the metalloporphyrin catalysts under different conditions. The catalyst seemed to exhibit selectivity in the reactions. The reaction for benzoic acid substrate and tetrahydrofuran as the solvent did not yield any reaction products as illustrated in the chromatogram shown in Figure 39. Another reaction that did not showed any sign of progress as illustrated in Figure 38, was the reaction between benzoyl peroxide, benzoic acid, tetrahydrofuran, and acetonitrile as the solvent. The only peaks expressed in the resulting chromatograms around retention time of 4, was unreacted benzoic acid. These two reactions were performed without any visible light. The same reaction was performed under a photochemical reactor with visible purple light, the reaction mixture contained benzoyl peroxide, benzoic acid, tetrahydrofuran, and the different metal substituted porphyrins. The reactions were analyzed through GC-MS and the results for this was tabulated and displayed in Table 5 as well as Figure 37. This time there were multiple products identified from the reactions. Analyzing the chromatograms, the results showed very similar results for all the metal substituted porphyrins. Some of the examples identified are biphenyl, terphenyl, benzoic acid phenyl ester, 2-phenyloxolane, and many more. The results indicate that the catalyst was coupling the aromatic rings to one another creating biphenyl and terphenyl as well as oxidizing the substrates making esters and carboxylic acid derivatives. Further exploring the reaction with benzoic acid and tetrahydrofuran, tert-butyl nitrite was added instead of benzoyl peroxide as an oxidant as shown in Table 8 and Figure 42, which show difference in the reactions. The replacement of benzoyl peroxide for tert-butyl nitrite created different product, yielding one major product, tetrahydro-2-methyl-2-furanol. The addition tert-butyl nitrite seemed to activate the tetrahydrofuran substrate by both coupling and oxidizing the compound. Another substrate that was used was trans-cinnamic acid (TCA). TCA was used

instead of benzoic acid and the results were tabulated in Tables 4,6,7, and 9. Trans-cinnamic acid was used in conjunction with tetrahydrofuran, benzoyl peroxide, the solvent acetonitrile along with the metal substituted metalloporphyrin catalysts and the results for this reaction is shown in Table 6 and Figure 40. GC-MS analysis shows the products to be biphenyl, benzene phenyl ester, stilbene, and phenyl-3-phenylpropanoate as seen in Table 6. Biphenyl is a common product in both the trans-cinnamic acid and benzoic acid, indicating that the catalyst on both reaction couple two phenyl molecules together. Stilbene is also another couple product indicating positive catalytic activity. The presence of benzene phenyl ester and phenyl 3-phenylpropanoate is an indication of oxidation and coupling of the aromatic rings. Table 7 shows the tabulated results of the reaction of trans-cinnamic acid, tetrahydrofuran, acetonitrile, and tert-butyl nitrite in the presence of the metal substituted porphyrins. This reaction was different because of the addition of tert-butyl nitrite instead of benzoyl peroxide. The results and products identified in the chromatogram in Figure 41 are as follows: tetrahydrofuran, styrene 2-nitroethylene, and trans-cinnamic acid. The major product in this reaction was styrene 2-nitroethylene indicating that tert-butyl nitrite is very selective in yielding a certain product and playing a major role in the reaction. A second part of this investigation included the oxidation of aldehydes to their corresponding carboxylic acids based on previous reported literature.[64-65] This reaction was done under oxygen bubbling and the mixture of aldehydes, metal substituted tetraphenyl porphyrin, and dichloromethane as a solvent were exposed to a photochemical reactor with purple light. The results for this photochemical reaction were tabulated and shown in Table 4 and the corresponding chromatogram in Figure 36. In this reaction the corresponding carboxylic acids of benzaldehyde and propionaldehyde were expected to be seen, the results showed propanoic acid, 3-methylbenzoic acid, 5-methyl-3-heptanol, 1-pentanol, and many long

carbon chain oxidized compounds. The oxidation of aldehydes was achieved by this reaction as well as possible coupling of carbon-carbon bonds to form long oxidized carbon chains.

CHAPTER V

CONCLUSION

The catalytic activity of tetraphenyl metalloporphyrin catalysts as possible photocatalysis was investigated. The tetraphenyl porphyrin ligand, TPP, was successfully coordinated with different divalent transition metals such as Co (II), Cu (II), Ni (II), and Pd (II). Powder X-ray diffraction characterization allowed for the determination of the metalloporphyrin crystal structures which resulted in a tetragonal structure present in all of the metal substituted porphyrins and its parent ligand. The free base porphyrin ligand was found to have both a tetragonal and orthorhombic crystal structure. X-ray diffraction also revealed the Cu (II) tetraphenyl porphyrin adopts a tetragonal and monoclinic crystal structure, which was consistent with the literature and coordination of metalloporphyrin.

UV-Vis and FT-IR spectroscopy allowed the determination and identifications of the absorption bands Soret (B) bands and Q bands as well as the vibrational functional groups associated with the metalloporphyrin catalysts, respectively. UV-Vis experimental results identified the absorption Soret bands as 421, 420, 418, 425, and 420 nm for H_2TPP, CoTPP, CuTPP, NiTPP, and PdTPP, respectively. The Q bands were also measured experimentally the results were as followed: H_2TPP shows Q bands at 518, 556, 594, and 654 nm; CoTPP shows Q bands at 525, 593, and 652 nm; CuTPP shows the Q bands at 503, and 543 nm; NiTPP shows Q bands at 532, 560, 622, and 658 nm; and finally PdTPP shows Q bands at 489, 528, 561, and 612 nm.

As previously discussed, the effect of the metal centered on the UV-Vis absorption spectra of porphyrin was analyzed and directly correlated to the nature of the metallic center and interaction with the porphyrin ligand (TPP) bonding orbitals following Gouterman's four orbital representation of HOMO and LUMO bonding orbitals. As described on the literature, the UV-Vis spectra changes are correlated to the change in symmetry of the porphyrin compound once the metal center is coordinated to the ligand, making the ligand TPP become more symmetrical due to the coordination associated with it. Furthermore, FT-IR analysis was performed in all synthesized catalysts and free base porphyrin ligand (TPP) and the results were tabulated in Table 1. The results show all the absorption vibrational bands for the functional groups of both the free base porphyrin, H_2TPP, and the Metalloporphyrin derivatives. As discussed, the most prominent vibrational stretching band is the N-H secondary amine band in the region of above 3300 cm^{-1}. This stretching vibrational band corresponds to the secondary amine present in H_2TPP and absent in the metalloporphyrin derivatives. The absence of this band is an indication of a successful coordination between the free base porphyrin ligand and the metal ion. Another observation associated with the coordination of the metal ion to the porphyrin ligand, H_2TPP, is the shift of the vibrational bands to higher or lower frequencies. This shift in the frequencies is directly related to the nature of the metal ion and the effects it has on the FT-IR spectra as seen in the experimental section as well as corroborated with the literature. Table 1 summarizes all the experimental frequencies as well as identified the functional groups stretches for H_2TPP, CoTPP, CuTPP, NiTPP, and PdTPP.

Finally, the synthesized compounds were the subject for possible photocatalytic reactions under a visible light photoreactor. The conditions of the reactions were very similar only differing in the catalyst, substrates, and oxidant. For a typical reaction, the appropriate

metalloporphyrin was dissolved in the solvent acetonitrile, the substrates such as aromatic carboxylic acid, benzoic acid or trans-cinnamic acid, were added, as well as the second substrate, tetrahydrofuran. To this mixture the presence of an oxidant, benzoyl peroxide or tert-butyl nitrite, was added as well. The progress of the reactions was recorded by sampling the reactions every hour and analyzing them through gas chromatography-mass spectroscopy. The tabulated results for the analysis and chromatograms are shown in tables 4-9 and figures 36-43, respectively. A second part of the catalytic study was the investigation of the oxidation of aromatic aldehydes to their corresponding carboxylic acids. The results proved this part of the investigation successful since all the corresponding carboxylic acids were seen in the chromatograms. The catalyst also had other effects on the reactions, oxidizing and coupling the substrates. This is both seen in the reactions of benzoic acid, trans-cinnamic acid, tetrahydrofuran and the aldehyde oxidation reaction. It is believed that the metal substituted porphyrins are activated by the photochemical light absorptions, exciting the catalyst, the relaxation to the ground state transfers the energy associated with the excitation to the substrates, catalyzing the reaction forward. This is evident on the results were there was no reaction such in Figure 38 and 39 in the absence of photochemical light. Examining the catalytic activities of each of the metalloporphyrin, the assumption can be made that all four catalyst behave very similar yielding almost identical results depending on the substrates and conditions of the reactions. There were instances where the palladium (II) and nickel (II) metal substituted tetraphenyl porphyrin were seen to achieve higher intensity for some of the products found, but for the most part each catalyst behaved almost the same expressing the same catalytic activity. This investigation was built on previous related works seen in literature, and the mission of this research was to further establish contribute to this metalloporphyrin research. Overall, the

research fulfilled the initial hypothesis that metalloporphyrin catalyst could be used as possible photocatalysts and could both under oxidative and reductive processes to catalyze reactions. This foundation was built on the abundant natural porphyrin complexes found in nature and their powerful roles in the most vital of chemical reactions in both animals and plants, alike. The powerful mimicking properties of the synthetic meso-tetraphenyl porphyrin and its metal substituted derivatives led and contributed to this investigation.

REFERENCES

1. Jiang, J.; Bekaroğlu, Ö. *Functional Phthalocyanine Molecular Materials*; Springer Science & Business Media, 2010.

2. Hosoowi, L; Kyeong-Im, H; Woo-Dong, J. Design and Applications of Molecular Probes Containing Porphyrin Derivatives. *Coord. Chem. Rev.* **2017,** 354, 46-73.

3. Vicente, M. G. H.; Smith, K. M. In Embryonic Encyclopedia of Life Sciences1999, Nature Publishing Group: London;www.els.net

4. Lesage, S; Xu, H; Durham, L. The Occurrence and Roles of Porphyrins in the Environment: Possible Implications for Bioremediation. *Hydrol. Sci. J.* **1993,** 38.

5. Francis, G.W. Pigments: Thin-Layer (Planar) Chromatography. **2000**.

6. Woods, J. *Porphyrin Metabolism as Indicators of Metal Exposure and Toxicity;* In: Goyer R.A.,Cherian M.G. (eds) Toxicology of Metals. Handbook of Experimental Pharmacology, vol. 115. Springer, Berlin, Heidelberg.

7. Treibs, A. Chlorophyll- und Häminderivate in Organischen Mineralstoffen. *Angew. Chem.* **1936,** 49.

8. Dechanie, G; Gray, M. Chemistry and Association of Vanadium Compounds in Heavy Oil and Bitumen, and Implications for Their Selective Removal [†]. *Energy Fuels.* **2010**, 24, 5, 2795–2808.

9. Treibs, A. Chlorophyll- und Häminderivate in bituminösen Gesteinen, Erdölen, Erdwachsen und Asphalten. Ein Beitrag zur Entstehung des Erdöls. *Justus Liebigs Ann. Chem.***1934,** 510.

10. Treibs, A. Chlorophyll- und Häminderivate in Organischen Mineralstoffen. *Angew. Chem.* **1936,** 49.

11. T, Lash. Synthesis of the Porphyrins from Petroleum. *Org. Geochem.* **1989,** 14, 2, 213-225.

12. Xu, H; Lesage, S. Separation of Vanadyl and Nickel Petroporphyrins on an Aminopropyl Column by High-Performance Liquid Chromatography. *J. Chromatogr. A*. **1992**, 607, 1, 139-144.

13. Fukuzumi, S; Lee, Y; Nam, W. Photocatalytic Redox Reactions with Metalloporphyrins. *J. Porphyrins Phthalocyanines.* **2020,** 24, 21-32.

14. Zhou, Q; Zou, Y; Lu, L; Xiao, W. Visisble-Light-Induced Organic Photochemical Reactions through Energy-Transfer Pathways. *Angew. Chem., Int. Ed.* **2019,** 58, 6.

15. Mandal T; Das, S; De Sarkar, S. Nickel (II) Tetraphenylporphyrin as an Efficient Photocatalyst Featuring Visible Light Promoted Dual Redox Activities. *Adv. Synth. And Catal.* **2019**, 361, 13.

16. Prier, C; Rankic, D; MacMillan, D. Visisble Light Photoredox Catalysis with Transition Metal Complexes: Applications in Organic Synthesis. *Chem. Rev.* **2013**, 113, 7, 5322–5363

17. Reiser, O. Opportunities for Visisble-Light-Catalyzed Atom Transfer Radical Addition Reactions and Related Processes. *Acc. Chem. Res*. **2016**, 49, 1990–1996.

18. Hossain, A; Vidyasagar, A; Eichinger, C; Lankes, C; Phan, J; Rehbein, J; Reiser, O. Visible-Light-Accelerated Copper (II)-Catalyzed Regio- and Chemoselective Oxo-Azidation of Vinyl Arenes. *Angew. Chem. Int. Ed.* **2018**, 57, 8288–8292.

19. Merrit, J; Loening, K; Dixon, H. Nomenclature of Tetrapyrroles. *Pure and Appl. Chem.* **1979**, 51, 2252-2304.

20. Kadish, K. M.; Smith, K. M.; Guilard, R. *The Porphyrin Handbook: Applications of Phthalocyanines;* Elsevier, 2003.

21. Kadish, K. M. *The Porphyrin Handbook*; Elsevier, 1999.

22. Okada, S; Segawa, H. Substituent-Control Exciton in J-Aggregates of Protonated Water-Insoluble Porphyrins. *J. Am. Chem. Soc***. 2003**, 125, 9, 2792–2796.

23. Brothers, P. Boron Complexes of Porphyrins and Related Polypyrrole Ligands: Unexpected Chemistry for both Boron and the Porphyrin. *Chem. Commun.* **2018.**

24. Lavell, D. A Review of: "Coordination Compounds of Porphyrins and Phthalocyanines. *Synth. React. Inorg. Met.-Org. Chem.* **1982**, 12, 3, 323-324.

25. Figueira, F.; M.R. Pereira, P.; Silva, S.; A.S. Cavaleiro, J.; P.C. Tome, J. *Curr. Org. Synth.* **2014**, 11, 1, 110–126.

26. Alves, E; Faustino, M; Neves, M; Cunha, A; Nadais, H; Almeida, A. Potential Applications of Porphyrins in Photodynamic Inactivation Beyond the Medical Scope. *J. Photochem. Photobiol. C Photochem. Rev.* **2015**, 22, 34-57.

27. Lu, H; Zhang, X. Catalytic C–H Functionalization by Metalloporphyrins: Recent Developments and Future Directions. *P. Chem. Soc. Rev.* **2011**, 40, 4, 1899-1909.

28. Knör, G. Recent Progress in Homogeneous Multielectron Transfer Photocatalysis and Artificial Photosynthetic Solar Energy Conversion. *Coord. Chem. Rev.* **2015,** 304-305.

29. Gale, P; Anzenbancher, P; Sessler, J. Calixpyrroles II. *Coord. Chem. Rev.* **2001**, 57-102.

30. Tsuda, A.; Osuka, A. Discrete Conjugated Porphyrin Tapes with a Exceptionally Small Bandgap. *Adv. Mater.* **2002**, *14* (1), 75-79.

31. Arnold, L.; Müllen, K. Modifying the porphyrin core – a chemist's jigsaw. *J. Porphyrins Phthalocyanines*. **2011**, *15*, 757-779.

32. Luck, R. L. Phthalocyanine materials synthesis, structure and function by Neil B. McKeown. *Mater. Manuf. Processes.* **1999**, *14* (3), 450-451.

33. Wright, J.D. *Encyclo. of Mat. Scien. and Tech. 2001, 6987-6991.*

34. Ulman, A.; Manassen, J. Synthesis of new tetraphenylporphyrin molecules containing heteroatoms other than nitrogen. I. Tetraphenyl-21,23-dithiaporphyrin. *J. Am. Chem. Soc.* **1975**, *97* (22), 6540-6544.

35. Paolesse, R.; Nardis, S.; Monti D.; Stefanelli, M.; Di Natale, C. Porphyrinoids for Chemical Sensor Applications. *Chem. Rev.* **2017**, *117* (4), 2517-2583.

36. Silvers S.J.; Tulinsky, A. J. The crystal and molecular structure of triclinic tetraphenylporphyrin. *J. Am. Chem. Soc.* **1967**, *89* (13), 3331-3337.

37. Fleischer, E. B. Structure of porphyrins and metalloporphyrins. *Acc. Chem. Res.* **1970**, *3* (3), 105-112.

38. Hoard, J. L.; Cohen, S.H.;Click, M.D. *J. Am. Chem. Soc*., 89, **1922 (1967).**

39. Scheidt, R.W.; *Accnts. Of Chem. Research*.**1977.**

40. Peterson, R.; Alexander, L. *J. Am. Chem. Soc.*, **1968,** 90, 3873.

41. Fischer, M.; Templeton, D; Calvin, M. American Crystallographic Association

Winter Meeting, **1969.**

42. E. Fleischer; R. Thorp, *Chem. Commun.,* **1969**, 475.

43. Bennett, W. E.; Broberg, D. E.; Baenziger, N. C. Crystal structure of stannic phthalocyanine, an eight-coordinated tin complex. *Inorg. Chem.* **1973**, *12* (4), 930-936

44. Rothemund, P. Formation of Porphyrins from Pyrrole and Aldehydes. *J. Am. Chem. Soc.* **1935**, *57* (10), 2010–2011.

45. Rothemund, P.; Menotti, A. R. Porphyrin Studies. IV.1 The Synthesis of α,β,γ,δ-Tetraphenylporphine. *J. Am. Chem. Soc.* **1941**, *63* (1), 267–270.

46. Adler, A. D.; Longo, F. R.; Shergalis, W. Mechanistic Investigations of Porphyrin Syntheses. I. Preliminary Studies on ms-Tetraphenylporphin. *J. Am. Chem. Soc.* **1964**, *86* (15), 3145–3149

47. Adler, A. D.; Longo, F. R.; Finarelli, J. D.; Goldmacher, J.; Assour, J.; Korsakoff, L. J. A Simplified Synthesis for Meso-tetraphenylporphine. *J. Org. Chem.* **1967**, *32* (2), 476.

48. Lindsey, J. S. Synthetic Routes to meso-Patterned Porphyrins. *Acc. Chem. Res.* **2010**, 43 (2), 300-311.

49. Lindsey, J. S.; Schreiman, I. C.; Hsu, H. C.; Kearney, P. C.; Marguerettaz, A. M. Rothemund and Adler-Longo reactions revisited: synthesis of tetraphenylporphyrins under equilibrium conditions. *J. Org. Chem.* **1987**, *52* (5), 827–836.

50. Yaseen, M.; Ali, M.; NajeebUllah, M.; Ali Munawar, M.; Khokhar, I. Microwave-assisted synthesis, metalation, and duff formylation of porphyrins. *J. Heterocycl. Chem.* **2009**, *46* (2), 251–255.

51. Liu, M. O.; Hu, A. T. Microwave-assisted Synthesis of Phthalocyanine-porphyrin complex and its Photoelectric Conversion Properties. *J. Organomet. Chem.* **2004**, *689* (15), 2450-2455.

52. Warner, M. G.; Succaw, G. L.; Hutchison, J. E. Solventless Syntheses of Mesotetraphenylporphyrin: New Experiments for a Greener Organic Chemistry Laboratory Curriculum. *Green Chem.* **2001**, *3*, 267.

53. RaeAnne E. Falvo, Larry M. Mink,Diane F. Marsh. Microscale Synthesis and 1H NMR Analysis of Tetraphenylporphyrins. *J. Chem. Educ*. **1999**, *76*, 237-239.

54. Adler, A. D.; Longo, F. R.; Finarelli, J. D.; Goldmacher, J.; Assour, J.; Korsakoff, L. J. A Simplified Synthesis for Meso-tetraphenylporphine. *J. Org. Chem.* **1967**, *32*(2), 476.

55. Fleischer, E.B.; Miller, C.K.; Webb, L.E. Crystal and Molecular Structures of Some Metal Tetraphenylporphines. *J. Am. Chem. Soc.* **1964**, *86* (12), 2342-2347.

56. Aziz, M.S.; El-Nahass, M.M.; Makhlouf, M.M.; Zeyada, H.M.; Spectrochemica Acta part. A; *Molec. And Biomolc. Spectr.* **2005**, *61*, 3026-3031.

57. Spellane, P.J.; Gouterman, M.; Antipas, A.; Kim, S.; Liu, Y.C. Porphyrins. 40. Electronic spectra and four-orbital energies of free-base, zinc, copper, and palladium tetrakis(perfluorophenyl)porphyrins. *Inorg. Chem.* **1980**, *19* (2), 386-391.

58. Hashimoto, T.; Choe, Y.; Nakano, H.; Hirao, K. Theoretical Study of the Q and B Bands of Free-Base, Magnesium, and Zinc Porphyrins, and Their Derivatives. *J. Phys. Chem.* **1999**, *103*, 1894-1904.

59. Namuangruk, S et al.; *Dalton Trans.* **2014**, *43*, 9166-9176.

60. Goc, J.; Ion, R.M.; Wrobel, D. *J. Mol. Struct.* **1998**, *61*, 239-246.

61. Marsh, D.F.; Mink, L.M. Microscale Synthesis and Electronic Absorption Spectroscopy of Tetraphenylporphyrin H2(TPP) and Metalloporphyrins ZnII(TPP) and NiII(TPP). *J. Chem. Educ.* **1996**, *73* (12), 1188.

62. The Medical Biochemistry Page; *Heme and Bilirubin Metabolism*, 2020.

63. Thomas, D.W.; Martell, A.E. Metal Chelates of Tetraphenylporphine and of Some p-Substituted Derivatives1,2. *J. Am. Chem. Soc.* **1959**, *81* (19), 5111-5119.

64. Naadeen, S et al.; *Rasayan J. Chem.* **2016**, 309-314.

65. Zhou, X. et al. Aerobic Oxidation of Benzylic Aldehydes to Acids Catalyzed by Iron (III) Meso-tetraphenylporphyrin Chloride under Ambient conditions. *Chin. Chem. Lett.* **2007**, *18*, 926-928.

66. Hajimohammadi, M.; Safari, N.; Mofakham, H.; Shaabani, A. A new and efficient Aerobic Oxidation of Aldehydes to Carboxylic Acids with Singlet Oxygen in the presence of Porphyrin Sensitizers and Visible Light. *Tetrahedron Lett.* **2010**, *51* (31), 4061-4065.

BIOGRAPHICAL SKETCH

Alexis Echavarria was born in 1992 in Veracruz, Mexico to Tereso Echavarria and Cira Trejo. He grew up half his life in Veracruz, Mexico. Then he moved to Port Isabel, Texas where he first attended Port Isabel Junior High School and Port Isabel High School, graduating in May 2011. After graduating high school, he attended the University of Texas at Brownsville where he pursued a bachelor's in science in Biology but did not complete it. Alexis attended the University of Texas Rio Grande Valley as a returning student in May 2015 to May 2018, where he completed a Bachelor of Science in Chemistry. Wanting to further advance his career, he enrolled again at the University of Texas Rio Grande Valley to work towards a Master of Science in Chemistry. At the University of Texas Rio Grande Valley, he worked mostly as a teaching assistant for the Chemistry department as well as doing research towards his graduate career in chemistry. Alexis graduated with a Master of Science in Chemistry in December 2020. Alexis Echavarria's permanent address is 311 East Monroe, Port Isabel, Texas 78578.